

# A photometric study of chemically peculiar stars with the *STEREO* satellites. I. Magnetic chemically peculiar stars<sup>★</sup>

K. T. Wraight,<sup>1†</sup> L. Fossati,<sup>1</sup> M. Netopil,<sup>2</sup> E. Paunzen,<sup>2</sup> M. Rode-Paunzen,<sup>2</sup>  
D. Bewsher,<sup>3</sup> A. J. Norton<sup>1</sup> and G. J. White<sup>1,4</sup>

<sup>1</sup>Department of Physical Sciences, Open University, Walton Hall, Milton Keynes MK7 6AA, UK

<sup>2</sup>Institut für Astronomie, Universität Wien, Türkenschanzstrasse 17, 1180 Wien, Austria

<sup>3</sup>Jeremiah Horrocks Institute, University of Central Lancashire, Preston, Lancashire, PR1 2HE, UK

<sup>4</sup>Space Science and Technology Department, STFC Rutherford Appleton Laboratory, Chilton, Didcot, Oxfordshire, OX11 0QX, UK

## ABSTRACT

About 10% of upper main sequence stars are characterised by the presence of chemical peculiarities, often found together with a structured magnetic field. The atmospheres of most of those chemically peculiar stars present surface spots, leading to photometric variability caused by rotational modulation. The study of the light curves of those stars therefore, permits a precise measurement of their rotational period, which is important to study stellar evolution and to plan further detailed observations. We analysed the light curves of 1028 chemically peculiar stars obtained with the *STEREO* spacecraft. We present here the results obtained for the 337 magnetic chemically peculiar stars in our sample. Thanks to the cadence and stability of the photometry, *STEREO* data are perfectly suitable to study variability signals with a periodicity typical of magnetic chemically peculiar stars. Using a matched filter algorithm and then two different period searching algorithms, we compiled a list of 82 magnetic chemically peculiar stars for which we measured a reliable rotational period; for 48 of them this is the first measurement of their rotational period. The remaining 255 stars are likely to be constant, although we cannot exclude the presence of long period variability. In some cases, the presence of blending or systematic effects prevented us from detecting any reliable variability and in those cases we classified the star as constant. For each star we classified as variable, we determined temperature, luminosity, mass and fractional age, but the limited statistics, biased towards the shorter periods, prevented us from finding any evolutionary trend of the rotational period. For a few stars, the comparison between their projected rotational velocity and equatorial velocity let us believe that their real rotational period might be longer than that found here and previously obtained. For the 82 stars identified as variable, we give all necessary information needed to plan further phase dependent observations.

**Key words:** techniques: photometric – catalogues – stars: chemically peculiar – stars: rotation

## 1 INTRODUCTION

About 10% of upper main sequence stars are characterised by remarkably rich line spectra. Compared to the solar case, overabundances are often inferred for some iron peak (e.g., Cr) and rare earth (e.g., Eu) elements, whereas some other chemical elements are underabundant (e.g., Sc). Some of these chemically peculiar (CP) stars also exhibit organised magnetic fields with a typical strength from a few hundreds up to few tens of thousands of Gauss. Chemically peculiar stars are usually subdivided into four groups: metallic line stars (CP1), magnetic Ap stars (CP2), HgMn stars (CP3), and

He-weak stars (CP4) (Preston 1974). Chemical peculiarities are due to the diffusion of the chemical elements, resulting from the competition between radiative pressure and gravitational settling, which in magnetic stars is guided by the magnetic field, possibly in combination with the influence of a weak, magnetically-directed wind (e.g., Babel 1992).

Several CP stars also display photometric variability, which is either due to pulsation or caused by rotational modulation. Some CP1 stars, falling inside the instability strip, display for example  $\delta$  Sct pulsation (Kurtz 1989), while rapid oscillations characterise some CP2 (ro Ap) stars (Kurtz 1982). Except for CP1 stars, diffusion leads to the formation of surface spots which produce photometric variability with the same periodicity as the stellar rotation period. The light curves of those stars can be fitted well by a sine

<sup>★</sup> Data obtained with the Heliospheric Imager instruments on board the *STEREO* spacecraft.

<sup>†</sup> K.T.Wraight@open.ac.uk

wave and its first harmonic, thus allowing recovery of the stellar rotation period with high precision.

Making use of photometric data obtained with the *STEREO* spacecraft, we analysed the photometry of 1028 stars listed in the Renson & Manfroid (2009) catalogue of known or suspected CP stars. This work presents the results obtained for the magnetic chemically peculiar stars (mCP stars: CP2 & CP4).

NASA's twin *STEREO* spacecraft aim primarily to study the solar corona in three dimensions and image Coronal Mass Ejections (CMEs) along the Sun-Earth line (Kaiser et al. 2008) but its data can also be used to gather high precision space photometry of background stars. As a matter of fact, photometry extracted from data obtained by the Heliospheric Imager (HI) on board the *STEREO*-Ahead spacecraft (Eyles et al. 2009) has already been used to produce a catalogue of eclipsing binary stars (EBs) (Wraight et al. 2011). The high photometric precision is ensured by the stability and accuracy of the calibration, as described by Brown et al. (2009) and Bewsher et al. (2010). In this work we use data obtained by both the Ahead *STEREO* spacecraft (*STEREO*/HI-1A) and the Behind spacecraft (*STEREO*/HI-1B) using a custom matched filter algorithm to extract the signals of variability.

The *STEREO*/HI-1 data have a cadence of about forty minutes and cover in total four and half years, where each data-block, herein referred to as an epoch, from each spacecraft covers about twenty days with gaps of about one year. Given the fact that most of the photometric variability of mCP stars has a periodicity between several hours and a few days, *STEREO* photometry is perfectly suitable for the detection and measurement of this periodic signal.

## 2 OBSERVATIONS AND ANALYSIS

### 2.1 Characteristics of *STEREO* data

The *STEREO*/HI-1 images have a field of view of 20 degrees by 20 degrees. The images, collected with a 2k x 2k pixel CCD, are binned on-board 2x2, returning to Earth images of 1k x 1k with a pixel scale of 70'' per pixel. All images use a single filter, with a spectral response mostly between 6300 Å and 7300 Å, although the bandpass does allow some light through around 4000 Å and 9500 Å (Bewsher et al. 2010). Figure 1 shows the HI-1A filter throughput, convolved with the CCD quantum efficiency, (dashed blue line) in comparison with synthetic spectral energy distributions (SED), calculated with LLMODELS (Shulyak et al. 2004), of two hypothetical stars of the same effective temperature ( $T_{\text{eff}}=8000$  K) and surface gravity ( $\log g=4.0$ ); one SED was calculated assuming classical mCP chemical peculiarities and a magnetic field of 10 kG (full black line), while the second SED was calculated assuming solar abundances and no magnetic field (dotted red line). It is important to notice that the amplitude of the variability, in the visible spectral range, of classical mCP stars decreases with increasing wavelength (Mikulášek 2007). For this reason, the window in the filter throughput around 4000 Å allows the *STEREO* photometry to be rather sensitive to the photometric variability of mCP stars.

As the primary purpose of the *STEREO* images is to observe coronal mass ejections (CMEs) along the Sun-Earth line, their field of view is centred 14 degrees away from the Sun's limb. Over the course of an orbit, almost 900,000 stars of 12th magnitude and brighter are imaged within 10 degrees of the ecliptic plane. The data very close to the brightest parts of the solar corona in the field of view can be affected by solar activity and this region was excluded from the analysis.

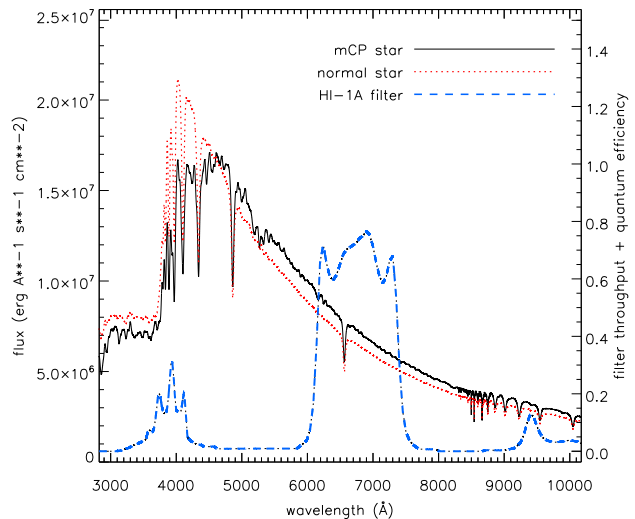


**Figure 1.** Synthetic spectral energy distributions calculated with  $T_{\text{eff}}=8000$  K and  $\log g=4.0$ , and assuming classical mCP chemical peculiarities and a magnetic field of 10 kG (full black line) and normal element abundances (dotted red line). The blue dashed line shows the HI-1A filter throughput, convolved with the CCD quantum efficiency, for which the scale is given by the y-axis on the right hand side of the plot.

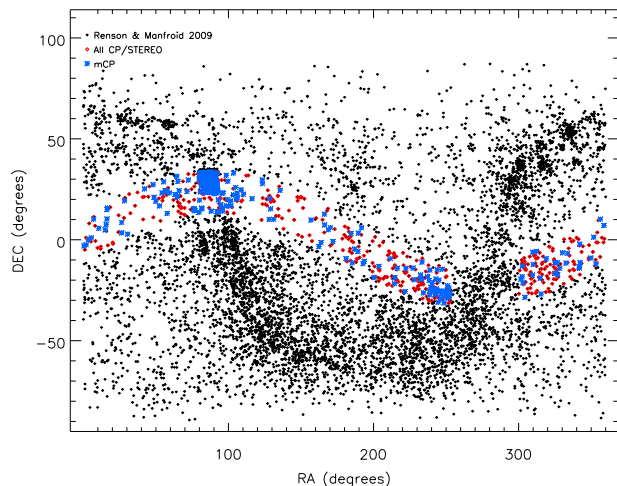


**Figure 2.** Black points show the position in the sky of all stars listed in the Renson & Manfroid (2009) catalogue. The red circles show the position of all 1028 CP stars present in the *STEREO* images. The blue asterisks show the position in the sky of the 337 mCP stars presented in this work. The clump of stars at RA~90 deg corresponds to the CP stars identified by Kharadze & Chargeishvili (1990). Right ascension and declination are given in degrees.

Figure 2 displays the position in the sky of all stars listed in the Renson & Manfroid (2009) catalogue, superimposed with the position of all 1028 analysed CP stars (red circles) and of the 337 mCP stars presented in this work (blue asterisks). Figure 2 shows clearly that we discarded from the analysis all CP stars close to the densely populated Galactic center. We applied this cut-off because of the strong blending in the *STEREO* images caused by the large pixel scale.

Figure 3 shows the CP2 star HD 147010 as seen by

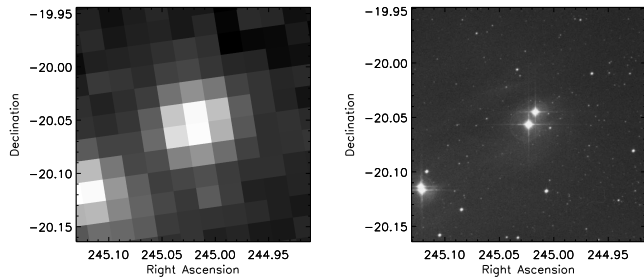


**Figure 3.** *STEREO*/HI-1A (left) and AAO *R* band (right) views of a visual binary consisting of the CP2 star HD 147010 and its slightly fainter neighbour HD 147009, illustrating the severity of blending with the 70'' pixel scale of the *STEREO*/HI-1 images.

*STEREO*/HI-1A in comparison with the image in the *R* band of the same region of the sky taken from the Anglo-Australian Observatory (AAO). It is not possible from the *STEREO* photometry alone to determine which of the two central stars is the source of the observed variability. This same problem is also present for other variables, for which a confirmation of the variability of a certain star requires additional data. In the particular case shown in Fig. 3, the nearby star is HD 147009, a bright ( $V=8.06$  mag) star with neither chemical peculiarities nor any known variability, thus the likely source of the observed signal is HD 147010.

The *STEREO*-Ahead spacecraft is in an Earth-leading orbit with a semi-major axis of about 0.95 AU, while the *STEREO*-Behind spacecraft is in an Earth trailing orbit with a semi-major axis of about 1.05 AU. This results in stars remaining in the field of view of the *STEREO*/HI-1A imager for just over 19 days and in the field of view of the *STEREO*/HI-1B imager for just over 22 days. The images have a cadence of 40 minutes. Figure 4 shows the light curve of the CP2 star HD 74521, illustrating the time separation between the different epochs of data, as well as some systematic effects which characterise a significant fraction of the *STEREO*/HI-1B data.

The *STEREO*/HI-1B data often exhibits sudden decreases in amplitude of all signals at a given time. These are attributed to errors in the background subtraction due to pointing changes resulting from micrometeorite impacts, as the *STEREO*/HI-1B imager is facing the direction of travel along the spacecraft's orbit. The severity of these events can range from a single observation point to days of erratic behaviour. Often we registered a marked decrease for some hours and then a return to the normality. Those systematics in the *STEREO*/HI-1B data can be easily recognized as such by visual inspection as these artifacts are erratically shaped and, importantly, aperiodic, whereas the classic variability of mCP stars is highly periodic.

The fact that the *STEREO*/HI-1A and *STEREO*/HI-1B satellites use slightly different photometric apertures and that the background subtraction does not take into account the number of stars in each field of view leads to a small difference between the magnitude of the same star obtained with the two satellites (Bewsher et al. 2010). For this reason we normalised the *STEREO*/HI-1B data to the same level as the steadier *STEREO*/HI-1A data with a detrending algorithm, described in Sect. 2.2.

## 2.2 Data analysis

Before being passed to a custom matched filter algorithm for analysis, all light curves are subjected to a culling routine to remove

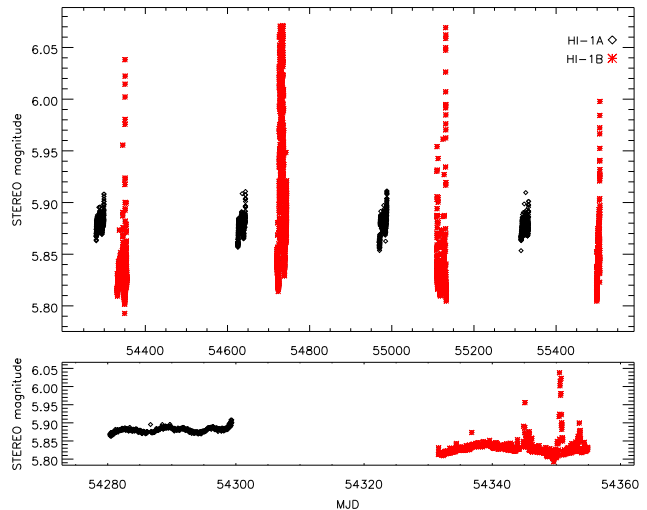


**Figure 4.** Untrended light curve of the CP2 star HD 74521. The black diamonds indicate the *STEREO*/HI-1A data-set and red asterisks indicate the *STEREO*/HI-1B data-set. As the two satellites progress in their orbits, the interval between *STEREO*/HI-1A and *STEREO*/HI-1B observations increases. Systematic effects from the *STEREO*/HI-1B are evident. The first block of *STEREO*/HI-1A and *STEREO*/HI-1B data is enlarged in the bottom plot.

some of the artifacts caused by Mercury and Venus passing through the field of view, as well as the more extreme pointing-related systematics present in the *STEREO*/HI-1B data, described in Sect. 2.1. This routine removes all data points more than 4 standard deviations away from the weighted mean magnitude. Polynomial detrending is then carried out using a 4th order polynomial in order to remove residual trends that may remain from the flat fielding or other artifacts. This removes some variability that is long compared to the length of an epoch, thus periods longer than about half the length of an epoch are not expected to be highly reliable. With the *STEREO* data, it is not possible to use differential photometry to avoid the detrending procedure, because trends are largely dependent upon the stars' location on the CCD, preventing differential photometry from being useful on a large scale. The *STEREO*/HI-1B data and also the succeeding epochs of *STEREO*/HI-1A data are also normalised to the same weighted mean magnitude as the first epoch of *STEREO*/HI-1A data.

The matched filter algorithm analyses a light curve in several stages, building model light curves and measuring the least-squared error of the model compared to the actual light curve. The model light curves consist of data points with the same time and errors as the real light curve. The matched filter algorithm works as follows:

- determine a best-fitting period. At this stage we adopted a sinusoidal shape, with an amplitude equal to three times the standard deviation, and produced the relevant periodogram.
- Fine-tune the period. A precise period is the most important step in the process and without this the other characteristics will not be reliably determined.
- Determine the amplitude of variability. This process is done before and after determining the best-fitting shape, with an amplitude resolution of 5 mmag.
- Determine the shape of the variability. A selection of shapes consisting of sinusoidal variability with different harmonic signals overlaid are used in addition to shapes based upon box-like total

eclipses, v-shaped eclipses and a composite of total eclipses with wide ingress and egress phases. The amplitude is recalculated after this stage and, if an eclipsing model was best-fitting, the algorithm also recalculates the duration and depth of the eclipses.

- If the best-fitting amplitude is zero this means that the model finds the star to be constant. The period obtained at the very first step of the algorithm is still returned.
- If an eclipsing model is best-fitting and the amplitude non-zero, eccentricity and amplitude of secondary eclipses are checked for. In this process, higher harmonics of the period are also checked.

This matched filter algorithm is processor-intensive and, depending on the number of data points (up to about 6000, currently), it may take from 5 to 10 minutes per star to process for a period range from 0.1 to 3.5 days with a resolution of 0.005 days ( $\sim 7$  minutes) initially, then fine-tuned to 0.00005 days ( $\sim 4$  seconds) in a narrow search around the best-fitting period. Higher frequencies were excluded to avoid the Nyquist frequency of about  $15.625 \text{ days}^{-1}$  (0.064 days). This was the period range used in the initial search, however the program showed during testing a clear preference for finding the half-period harmonic of EBs, to the extent that it was specifically programmed to check at double and triple the periods initially found to see if these produced a better fit. A second search was then done with periods up to 10 days using *STEREO*/HI-1A data only, as in some cases the *STEREO*/HI-1B data was of too poor quality to allow even strong variability to be detected. This particular upper limit of 10 days was chosen to avoid running into systematic errors from the polynomial detrending at about one half of the length of an epoch.

The periodograms and light curves (phase-folded on the best fitting period) produced by the matched filter algorithm were visually inspected, primarily to extract from the sample the objects which appeared clearly constant. Additionally, we classified as constant the stars which were so faint that any signal would be likely due to noise or if systematic effects were so extreme that the data were unusable, mostly stars at the very edge of the CCDs. The same classification was given to the stars for which the lack of data prevented the reliable detection of any variability. The list of those 133 stars is given in Table 1. The remaining 205 mCP stars that we did not consider definitely constant, or which merited further investigation on the basis of their features in the periodogram, were all individually examined in detail.

The first stage in this detailed analysis was to check the surrounding stars, within 8 pixels, as seen with the *STEREO*/HI-1A images, looking for signs of variability so that the risk of blending for each star could be understood. These stars have the potential for their signal and/or period to be affected by blending. The effects of blending can be broadly assigned to three different categories. *i*) Extreme cases where the target might not be the source of the variability and there is an equal chance the source may instead be a nearby star. *ii*) Severe cases where the target may be variable but there may be one or more other variables nearby and the true period has been distorted by the interference. *iii*) Minor cases where the target is clearly variable and no variability, or only vague variability, is seen in nearby stars and the only possible effect is a slight distortion of the period. Due to the *STEREO*/HI-1 pixel scale, most stars come into the latter category to some extent but the accuracy of the photometry precludes adjacent stars more than four magnitudes fainter from having a measurable influence. Thanks also to the different photometric apertures between the two satellites, the presence of a difference between the variability extracted from the *STEREO*/HI-1A and the *STEREO*/HI-1B data also indicates the

presence of blending. This method proved to be particularly helpful in assigning the source of variability for some blended stars. The 8 pixel range was chosen partly to be conservative, as blending effects have not been observed from such a distance, and partly to help trace whether a star closer than this to the target is genuinely variable or itself blended with a more distant neighbour.

The second stage in the detailed examination was an inspection of the detrended light curve of the target, using both *STEREO*/HI-1A and *STEREO*/HI-1B data, where available. In particular, we examined the severity of artifacts present in the *STEREO*/HI-1B data, deciding carefully where to “clean” the light curves to avoid obscuring or distorting a potential signal. For systematic effects, most commonly artifacts of the polynomial detrending, the severity can range from introducing a completely false signal to a small risk of distorting the period of an existing signal.

To attempt to remove remaining systematics, a 7th order polynomial was applied after the initial culling of outliers. This was sufficient to remove most of the effects of planetary incursions by Mercury and Venus. In extreme cases, it was necessary to remove entire epochs or even completely exclude *STEREO*/HI-1B data from the analysis, however some stars only needed a few clear outlying points removing and most only required minor cleaning, typically for small numbers of events due to pointing errors as described in Sect. 2.1.

The final stages of the detailed analysis were undertaken with Peranso<sup>1</sup>. We undertook the period search with two algorithms, to cross-check each other and avoid duplicating weaknesses. In each case, we searched periods between 0.1 and 10 days, although in a few individual cases a search was made outside this range. The Lomb-Scargle method (Scargle 1982) was employed in the period domain and the phase dispersion minimisation (PDM) method (Stellingwerf 1978) was employed in the frequency domain. We then examined the significant features in the periodogram produced with each method to extract the most likely period, its uncertainty and the epoch of the first maximum in the *STEREO* light curve.

### 3 RESULTS

Following the procedure described in Sect. 2.2, we compiled Table 2, listing the 122 stars we classified as constant after the detailed individual analysis, and Table 3, listing the 82 stars we classified as variable. Those tables, together with Table 1, present the main results of this work on the mCP stars. Each table lists the star name and the Renson & Manfroid (2009) identification number in the first two columns. The third and fourth columns list the coordinates of each star (in deg), while the average magnitude in the *V* band is given in the fifth column. Column number 6 lists the spectral classification and chemical peculiarity given by Renson & Manfroid (2009), while the seventh column lists the CP classification. The starting point for the critical assessment of the literature about the CP classification of our programme stars was the Catalogue of Ap, HgMn and Am stars by Renson & Manfroid (2009). They collected all objects which were reported as “peculiar” in the literature and list an approximate spectral type. Because at least classification resolution spectroscopy is necessary to establish the true nature of a peculiar object (e.g. Pausen et al. 2011), we used the relevant extensive catalogue by Skiff (2010) to verify all spectral types. If contradicting classifications were found, a

<sup>1</sup> <http://www.peranso.com>

question mark was set. The CP classification given in these Tables does not take into account the findings of this paper and is based only on the information given in the literature.

As mentioned in Sect. 2.2, Table 1 lists all stars that were immediately classified as constant, but it also includes stars for which the photometry was clearly affected by systematic effects and/or by blending, making the detection of any periodicity impossible. In particular, in Table 1, for all stars brighter than  $V \sim 5$  mag, the presence of systematic effects prevented us from detecting any periodic signal. Similarly, unless an exceptionally strong signal was present, the quality of the data did not allow us to conclude anything about stars fainter than  $V \sim 10.5$  mag. As a consequence, all stars listed in Table 1, with a magnitude between about 5 and 10.5 are either constant, or variable with a periodicity shorter/longer than 0.1/10 days, or variable with an amplitude below our sensitivity.

As mentioned before, Table 2 lists the stars that after individual analysis we either classified as constant, or for which systematics or blending prevented us from detecting reliable signals. Column 10 gives the particular reason for a certain star to be listed in this table: C when we concluded the star was constant<sup>2</sup>, B and S when respectively blending and systematics were too severe to allow the detection of a reliable signal. In a few cases we detected rather weak signals, with a small significance (see below). For those stars we added a W in column 10 and the period (in days) with its uncertainty (in days) respectively in columns 8 and 9. Those periods have to be taken with caution. In column 11 we finally listed the period found in the literature.

In Table 3 we list the objects for which we found and measured a genuine period (in days), listed in column 8, together with the period uncertainty (in days) in column 9 and the MJD of the epoch of the first recorded maximum in column 10. As shown in columns 8 and 9, in some cases we detected more than one significant period. As for Table 2, in the 11th column we included a remark indicating the possible presence of blending (B) or systematic (S) effects which could have slightly distorted the given value of the period. For those stars, marked with B and/or S, the effects of blending and systematics were not large enough to doubt the source of the variability. In column 11, we put an additional asterisk “\*” to highlight the stars for which we obtained an exceptionally strong signal. Column 12 lists the period found in the literature.

For each star in Table 3 we produced a periodogram (Fig. 11) and a phase-folded light curve (Fig. 12). The periodograms were produced using one of the outputs of the PDM method, called  $\Theta$ , defined in Stellingwerf (1978). Given the large number of photometric points,  $\Theta$  gives a direct indication of the significance of a certain period (see Eq. 13 in Stellingwerf 1978), which we then defined as the deviation from the median value of  $\Theta$  in units of standard deviations. All periods obtained for the stars that were genuinely variable have a significance larger than 7, where the maximum value is reached for HD 19832 (SX Ari) with a significance of about 32. In Table 3 we decided not to include the significance of the period because it is not the only factor which played a role in deciding whether a certain period was real or not; external factors, blending in particular, had to be taken into account, making the statistical significance misleading.

Figure 5 shows the phase-folded light curve (top) and the periodogram (bottom) for HD 19832 (SX Ari), for which the de-

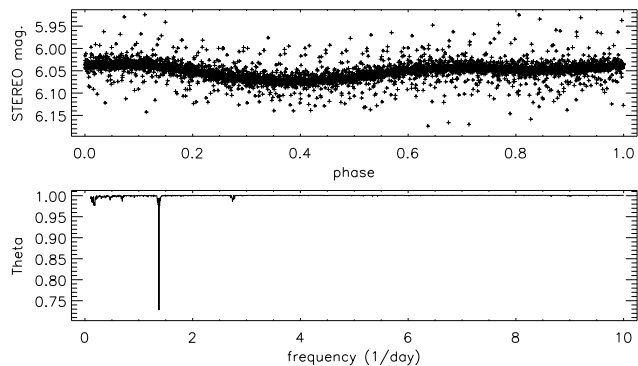


**Figure 5.** Top: light curve obtained for the CP2 star HD 19832 phase-folded with the most significant period of 0.7279 days. The periodogram is shown in the bottom panel. This mCP star is clearly variable and is listed in Table 3.

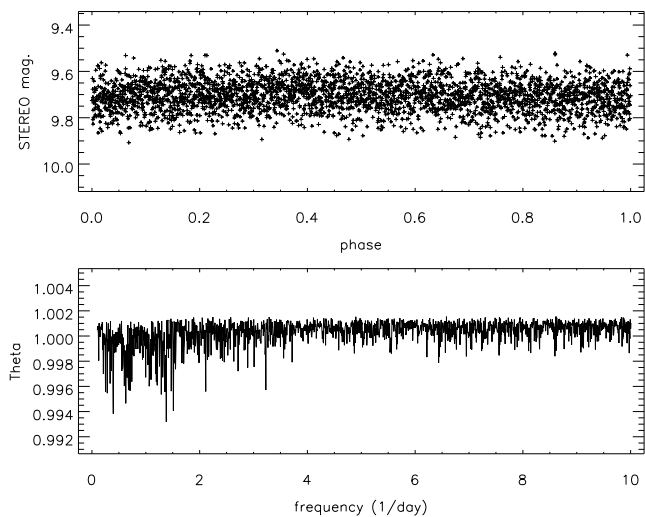


**Figure 6.** Same as in Fig. 5, but for HD 149228. For this mCP star, listed in Table 2, we did not obtain any significant period, meaning that the star is either constant or has a rotation period longer than 10 days. In this case the light curve is phase folded on the period given by the most significant peak in the periodogram (1.5066 days).

ripped period presents the strongest signal in our sample. In Fig. 6 and in Fig. 7 we show the periodogram and the phase-folded light curve for HD 149228 and HD 150035, respectively a star we classified as constant and a star for which we found a weak signal (see Table 2). HD 150035 is probably the most border-line case in our sample. The period stated in Table 2 has a significance below 7 and it does not match the previously known period given by Catalano & Renson (1998), although this is a rather bright star and neither blending nor systematics affect the photometry, as shown by the neatness of the phase-folded light curve. It is also possible that the amplitude of the variability is below the sensitivity of the instrument.

A handful of stars listed in Table 2 and 3, for which we measured a period, are the primary component of a spectroscopic binary system, e.g. HD 68351. For each of them, we did not find any relation between the orbital period of the binary system, given by Pourbaix et al. (2004), and the period obtained from the *STEREO* photometry. Figure 8 shows a comparison between the periods derived

<sup>2</sup> This means that the star is either constant, or variable with a periodicity shorter/longer than 0.1/10 days, or variable with an amplitude below our sensitivity, or pole-on.

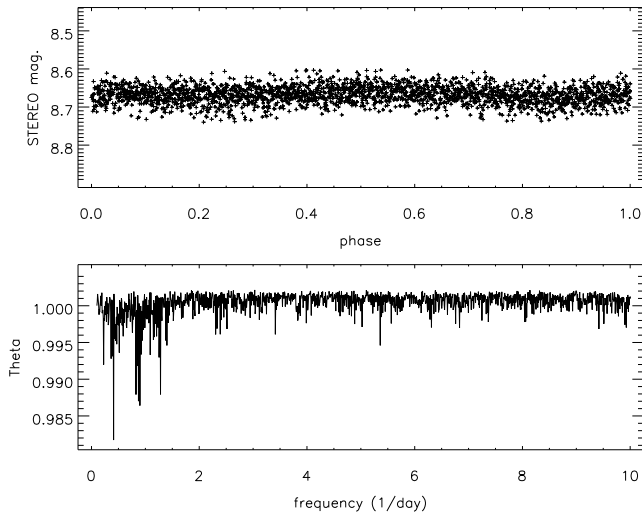


**Figure 7.** Same as in Fig. 5, but for HD 150035 and phase-folded on a period of 2.3389 days. This star is a border-line case (see text for more details).

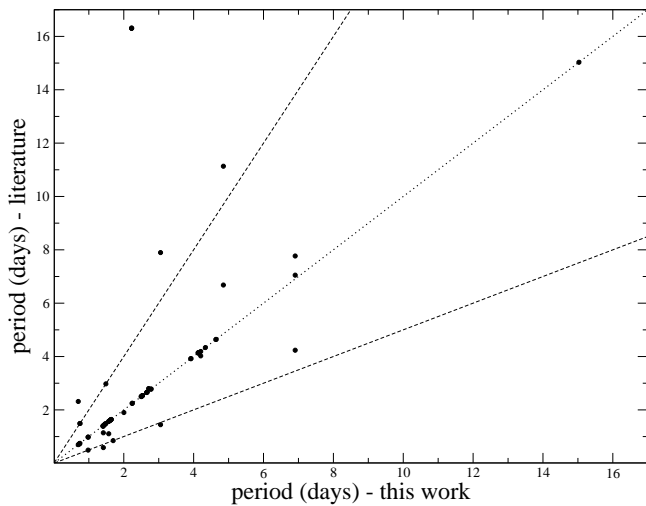


**Figure 8.** Comparison between the periods of mCP stars derived from the *STEREO* data and present in the literature. The dotted line shows the one-to-one relationship, while the dashed lines indicate the relationships relative to twice and half of the literature period.

from the *STEREO* data and those found in the literature. We register a general good agreement, except for the cases when the *STEREO* period is a harmonic of the one given in the literature, as for HD 12447<sup>3</sup>. Table 3 shows that this also happens quite often among the various periods present in the literature. The largest discrepancy is obtained for HD 111133 where the literature period is about 7.3 times larger than the one we obtained. In this case the published  $\sim 16$  days period is hardly recognisable in our data; a weak peak in the periodogram at a period just below 16 days, was found as in this case we extended our period search to more than 10 days to look for the period given in the literature. In our periodogram, the  $\sim 2.2$  days period gave the strongest signal, with a significance of about 8.

<sup>3</sup> This star is also a blend with the possible CP1 HD 12446.

### 3.1 Notes on individual stars

The stars HD 965, HD 142250, HD 209051, and HD 216018, confirmed as magnetic by previous spectropolarimetric measurements (Bychkov et al. 2009; Kudryavtsev et al. 2008; Romanyuk & Kudryavtsev 2008, , respectively), are listed among the constant stars in Table 1. For those objects our periodogram did not show any significant peak in the 0.1–10 days period range, meaning that their rotation period is likely to be longer than 10 days. For these four stars the rotation period is not known.

For the stars HD 26571 and HD 134214, listed in Table 1, Catalano & Renson (1998) and Renson & Catalano (2001) gave very different periods. For HD 26571, Catalano & Renson (1998) gave a period of 1.06 days, while Renson & Catalano (2001) gave a period of 15.749 days. Our periodogram did not show any significant peak around the 1 day period, therefore we presume that the 15.749 days period, given by Renson & Catalano (2001) is the correct one. Adelman (2008) confirmed the longer period and refined it to 15.7505 days. For HD 134214, Catalano & Renson (1998) gave a period of 248 days, while Renson & Catalano (2001) gave a period of 4.15 days. Our periodogram did not present any significant peak around 4 days, meaning that the longer period is more likely to be the correct one.

For the star HD 27295, listed in Table 1, Catalano & Renson (1998) reported a rotation period of 4.42 days, but our periodogram did not present any statistically significant period and also the detrended light curve did not show any sign of variability. Since the star has been confirmed to be magnetic, it is possible that the rotation period is longer than 10 days. Samus et al. (2009) listed the star HD 17471 (see Table 1) as a variable of the  $\alpha 2$  CVn type, without giving any period. Our light curve for this star is distorted by systematic effects, therefore we cannot provide a measurement of the rotation period.

Except for the very bright and very faint stars, for which systematic effects prevented us from detecting the presence of genuine variability, for the remaining objects listed in Table 1 we did not detect any significant period. For those stars there is no spectroscopic and/or polarimetric confirmation of their magnetic nature. We believe that most of those objects are either CP1 or chemically normal stars, while it is possible for some of them to be mCP stars with a rotation period longer than 10 days, or variable with an amplitude below our sensitivity.

For the mCP stars HD 47103 and HD 148321 (see Bychkov et al. 2009), listed in Table 2, we did not find any significant variability, although the data did not present any systematic effect and the photometry was not affected by blending. Most likely the rotation period of these two stars is longer than 10 days. Blending prevented us from detecting any reliable and significant variability for the mCP stars (see Bychkov et al. 2009) HD 22374, HD 23387, and HD 51688, also listed in Table 2.

For the magnetic stars HD 224926, HD 125248, and HD 150035 (see Bychkov et al. 2009), listed in Table 2, we identified a periodicity with a significance between 5 and 7, where for the first and second stars respectively, blending and systematic effects prevented us from obtaining a period convincing enough to include them among the certainly variable mCP stars. The period we measured for HD 125248 is in agreement with the one previously reported by Renson & Catalano (2001).

Renson & Catalano (2001) listed a rotation period of 1.563 days for GSC 00742-02169, while we obtained a significant period at 1.4828 days, which might have been distorted by blend-

ing. In Table 2 we listed the stars HD 10809, HD 250027, and HD 146998 as constant, although a previous period was reported by Kraus et al. (2007), Samus et al. (2009), and Catalano & Renson (1998), respectively. For both HD 10809 and HD 146998 we have not found any significant peak in the periodogram around the previously reported period values. For HD 250027 the period given by Samus et al. (2009) of about  $\sim 20$  days is out of our detectability window.

For the stars HD 1758, GSC 02390-00208, and AAO+27 25, listed in Table 2, we identified a peak in the periodogram which is considered not significant enough to classify these objects as certainly variable. We came to the same conclusion for the stars HD 23850, HD 23964, HD 242692, GSC 02403-00597, AAO+27 185, HD 39865, AAO+30 338, HD 48953, BD+23 1580, GSC 01398-00532, HD 118054, HD 138426, HD 139160, HD 144748, HD 151941, HD 215766, and HD 215913, but for those objects blending and/or systematic effects might have distorted the measured period. For these stars, there is no spectroscopic and/or polarimetric confirmation of their magnetic nature. HD 196470 is a magnetic roAp star for which blending prevented detection of any significant peak in the periodogram. Similarly, HD 206088 is a mCP star for which systematic effects did not allow us to measure any reliable period. For both HD 196470 and HD 206088 it is possible that their rotation period is longer than 10 days, or variable with an amplitude below our sensitivity.

For the remaining stars listed in Table 2 there is no spectroscopic and/or polarimetric confirmation of their magnetic nature and most of those objects are likely to be either CP1 or chemically normal stars, with a minority of mCP stars with a period longer than 10 days, or variable with an amplitude below our sensitivity.

About half of the stars we classified as variable and listed in Table 3 are known mCP stars and for some of them the rotation period has been previously measured. For those stars the results provide either a confirmation or a refinement of the previously known period, with the addition of a period uncertainty and of an epoch of maximum brightness, which is crucial information to plan spectroscopic observations aiming to perform, e.g., Doppler imaging. It is important to notice that blending and/or systematic effects, reported in column eleven of Table 3, could have slightly distorted the given period. For a few stars we registered also the presence of more than one significant period in the periodogram, which we reported in Table 3.

For the remaining 48 stars, listed in Table 3, the results represent the first measurement of their rotation period. In particular, very little is known for most of them and the clear detection of rotational variability is strongly suggestive of the presence of a structured magnetic field, chemical peculiarities and surface spots, although some of them might be CP3 stars, and therefore not magnetic. It would be extremely valuable to obtain spectropolarimetric observations for those stars, which could be quickly performed with instruments such as ESPaDOnS at the Canada-France-Hawaii Telescope (CFHT). In particular, given the average magnitude of those stars and because their magnetic field (if present) should be of the order of a few hundreds of Gauss, their detection will not require spectra with a large signal-to-noise ratio and therefore, such observations could be performed with short exposure times.

For the stars HD 43819 and HD 130559 we reported values of the rotation period longer than 10 days, adopted as maximum for the matched-filter algorithm. For HD 43819 we looked intentionally for a period around 15 days, because Renson & Catalano (2001) reported a period of 15.03 days. On the other hand, for HD 130559 the possible presence of a period longer than 10 days

appeared from the undetrended light curve, nevertheless, this value of the period has to be taken with caution.

## 4 DISCUSSION

For each star, listed in Table 3, we compiled Johnson *UBV*, Strömgren, and Geneva photometry from the General Catalogue of Photometric data (Mermilliod et al. 1997) and the additional literature to derive the effective temperature on the basis of the calibrations given by Netopil et al. (2008). These calibrations can be applied because they are specifically tuned for the different types of CP stars. The final  $T_{\text{eff}}$ , given in column 15 of Table 3, is the average  $T_{\text{eff}}$  obtained calibrating the different colors, while the standard deviation and the number of averaged temperatures are given in parentheses. When available, we adopted the spectroscopic  $T_{\text{eff}}$  listed in Netopil et al. (2008), and these cases are indicated with a “99” instead of the number of averaged temperatures. To each star, with a determined  $T_{\text{eff}}$ , we associated a further fixed uncertainty of 500 K for the CP2 stars and of 700 K for the CP4 stars, as proposed by the reference above (see also the discussion in Landstreet et al. 2007). For the following analyses we then adopted the largest uncertainty between the standard deviation and the fixed uncertainty.

For some stars later than spectral type A0 without Strömgren photometry, we were not able to determine individual reddening values based on the available photometry (see the discussion in Netopil et al. 2008), hence the determination of  $T_{\text{eff}}$  would be rather erroneous. In order to also obtain temperatures for these (CP2) objects, we made use of the spectral energy distribution (SED) fitting tool by Robitaille et al. (2007), which to some extent allows the extinction to be set as a free parameter. As input data we used the available *UBV* photometry or Geneva measurements transformed to *UBV* using the calibration by Harmanec & Božić (2001), in combination with 2MASS data (Cutri et al. 2003). Although the *U* magnitude is important for a proper fit of the energy distribution, the SED fitting was also applied to four objects without this filter information using *B* and *V* data taken from the ASCC-2.5 V3 catalogue (Kharchenko 2001). However, since for these stars a distance is available, a restriction of extinction was made using the three dimensional extinction maps by Arenou et al. (1992) in combination with the dust maps by Schlegel et al. (1998). Since the anomalous colours of CP objects have to be taken into account, a correction of the SED results is probably necessary. Therefore, we also processed the CP2 “standard” stars given in Netopil et al. (2008) in a similar way and determined the relation:

$$T_{\text{eff}} = 1032(167) [K] + 0.873(16) [K] T_{\text{SED}}, \quad (1)$$

with a correlation coefficient  $R = 0.990$  using in total 62 objects, valid for the temperature range 7500–15000 K.

The obtained (SED) reddening was finally applied to the available photometry of our programme stars to obtain an additional second temperature estimate, which was averaged. These results are in good agreement with the known spectral types, and are indicated with “50” in column 15 of Table 3, instead of the number of averaged temperature determinations. We could not apply this method to stars for which neither a parallax nor a *U* magnitude were available. These objects were detected by Kharadze & Chargeishvili (1990), the only available reference for most of them.

For the stars for which a parallax is present in the HIPPARCOS catalogue presented by van Leeuwen (2007), we determined the luminosity ( $\log L/L_{\odot}$ ) on the basis of the Johnson *V* magnitude, the bolometric correction given by Netopil et al. (2008), and the

interstellar reddening  $E(B - V)$  determined via the different photometric systems (see Netopil et al. 2008, for details) or via SED fitting, using a total-to-selective absorption ratio of  $R = 3.1$ . Table 3 lists in column 16 the derived luminosities with the relative uncertainties given in parentheses.

For all stars for which we derived  $T_{\text{eff}}$  and luminosity, we determined stellar mass and fractional age ( $\tau$  - fraction of main sequence lifetime completed) using the evolutionary tracks for solar metallicity given by Schaerer et al. (1993). Table 3 lists in columns 17 and 18 respectively the derived masses and fractional ages with the relative uncertainties in parentheses. In Table 3, the stars for which the mass is marked with a “Z” or “T” lie below the zero age main sequence (ZAMS) or above the terminal age main sequence (TAMS). In these cases the mass was estimated as the star would lie directly on the ZAMS or TAMS and the fractional age has then been set to 0 (ZAMS) or 1 (TAMS), without uncertainty. Stars for which a temperature is available but no parallax, were placed in the middle of the main-sequence band to obtain at least a rough mass estimate; for these objects no luminosity and fractional age is given in Table 3.

Bagnulo et al. (2006) showed that for field stars important age uncertainties arise from the use of isochrones with an inaccurate metallicity, especially for stars in the first half of their main sequence lifespan. The introduction of the fixed uncertainties on  $T_{\text{eff}}$  of 500 K for CP2 and 700 K for CP4 stars alleviates this problem. On the other hand, the use of tracks with an inaccurate metallicity has a much smaller impact on the derived masses.

The uncertainties given in Table 3 for the fractional ages are quite uniform in  $\tau$ , with an average of  $\sim 0.2$ . Landstreet et al. (2007) compared the uncertainties they obtained for the fractional ages for a set of mCP stars in open clusters with the ones given by Kochukhov & Bagnulo (2006) in a set of field mCP stars. Landstreet et al. (2007) concluded that the uncertainties given by Kochukhov & Bagnulo (2006) were probably underestimated, due to the small uncertainties adopted for  $T_{\text{eff}}$ . In this work we adopt temperature uncertainties similar to those used by Landstreet et al. (2007), making our uncertainties on the fractional ages more realistic compared to those of Kochukhov & Bagnulo (2006).

Figure 9 shows the position in the Hertzsprung-Russell (HR) diagram for all stars listed in Table 3 and for which we derived both  $T_{\text{eff}}$  and  $\log L/L_{\odot}$ . Figure 9 shows also the evolutionary tracks (Schaerer et al. 1993) adopted to derive the stellar masses and fractional ages. As expected, the CP4 stars are on average hotter and more luminous than the CP2 stars. Within the uncertainties, the position of the stars in the HR diagram is well inside the limits given by the ZAMS and TAMS, except for HD 107452, which lies more than  $2\sigma$  below the ZAMS and is likely connected to a problem with the adopted distance. HD 107452 is one of the closest objects of our sample, according to Hipparcos parallaxes. However, it is part of a close visual double star, probably influencing the parallax measurements. As a matter of fact, using the distance of 159 pc given by Gomez et al. (1998), which is more than twice of the Hipparcos one, the star would fall close to the ZAMS.

In Table 3 five stars (HD 142301, HD 142990, HD 145501, HD 146001, and HD 147010) belong to the Upper Sco association and are present in the work by Landstreet et al. (2007), who derived  $T_{\text{eff}}$ ,  $\log L/L_{\odot}$ ,  $M/M_{\odot}$ , and  $\tau$  for those stars. The agreement obtained for  $T_{\text{eff}}$ ,  $\log L/L_{\odot}$ , and  $M/M_{\odot}$  is remarkably good, being almost always less than  $1\sigma$  away from the previous value, while we notice relevant discrepancies for the fractional ages. We derived the fractional ages without considering the possible membership of open clusters or associations, while Landstreet et al. (2007) used

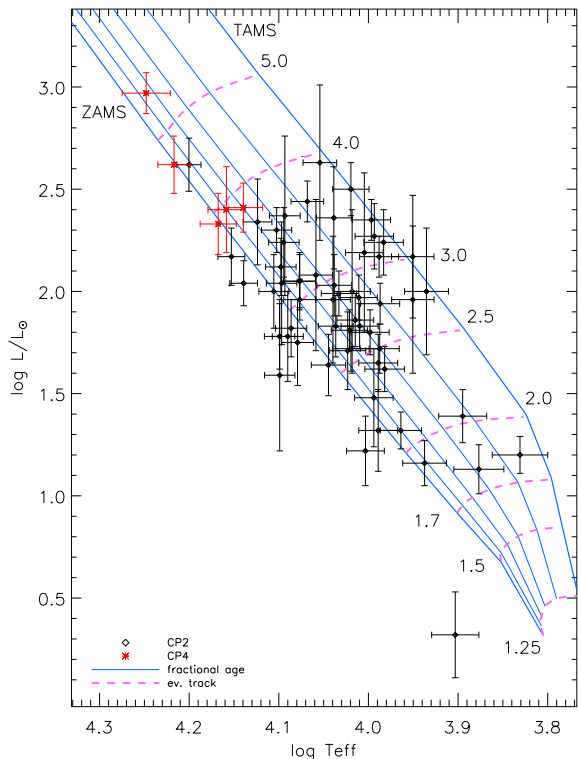


**Figure 9.** Hertzsprung-Russell diagram for the CP2 (black diamonds) and CP4 (red asterisks) stars listed in Table 3 and for which we derived both  $T_{\text{eff}}$  and  $\log L/L_{\odot}$ . The blue lines represent the lines of equal fractional age (Schaerer et al. 1993). The ZAMS and TAMS are indicated in the plot and highlighted with a thicker line. The dashed violet lines represent the main sequence evolutionary tracks used to derive the stellar masses. The stellar mass, relative to each track, in units of solar masses, is indicated in the plot. Both isochrones and evolutionary tracks are for solar metallicity.

this information to nail down the fractional age, sometimes to a few %. This shows clearly the advantage of using open cluster stars, for which the age is precisely known, to study stellar evolution. However, we have to note that the individual Hipparcos distances for the stars in the Upper Sco association are on average 10% larger than the mean distance adopted by Landstreet et al. (2007). This fact together with the adoption of a different temperature calibration (especially for CP4 objects) leads to a shift to larger fractional ages.

Kochukhov & Bagnulo (2006) compiled the values of the average quadratic longitudinal field, rotational period, and evolutionary status for about 200 mCP stars. From the point of view of the evolution of stellar rotation, their results indicate evidence for an increase of the stellar rotational period with increasing age, as a consequence of the conservation of angular momentum, which was previously shown also by North (1998). Unfortunately, our sample is too small and in particular biased towards shorter periods to be able to confirm or disprove Kochukhov & Bagnulo (2006)’s findings. Clearly, a thorough analysis of the evolution of the rotation period in mCP stars requires a large sample of open cluster stars.

In column 13 of Table 3 we added also the values of the average quadratic effective magnetic field, in Gauss. Those values have been taken from Bychkov et al. (2009), Kudryavtsev et al. (2008), and Romanyuk & Kudryavtsev (2008). When available, in



column 8 of Table 1, in column 12 of Table 2, and in column 14 of Table 3 we added the average projected rotational velocity ( $v \sin i$ ) values, put together on the basis of the compilation by Glebocki & Gnacinski (2005). Newer observations were included from catalogues and papers found in the CDS/Simbad databases. Values of upper and lower limits as well as uncertain ones were discarded resulting in a few thousands of individual data points. The averages were calculated using the published errors as reciprocal weights. If no errors were listed, we set it to 15%, which is a widely used value for such measurements.

As a test for the validity of the determined effective temperatures, luminosities, and rotational periods we calculated the equatorial velocities ( $V_{\text{eq}}$ ) from the formula of the oblique rotator model (see e.g. North 1998):

$$V_{\text{eq}}[\text{km s}^{-1}] = 50.6 R[R_{\odot}] / P[\text{days}] \quad (2)$$

where we calculated the stellar radii from  $T_{\text{eff}}$  and  $\log L/L_{\odot}$ . Figure 10 shows the comparison between the observed  $v \sin i$  and the computed  $V_{\text{eq}}$  for the stars listed in Table 3. As expected, taking into consideration the  $v \sin i$  uncertainties, most of the stars fall below the equality line ( $\sin i \leq 1$ ). For the stars which fall instead above the equality line it is possible that the calculated radius is too large or that the measured rotational period is too small. By calculating the surface gravity ( $\log g$ ), from  $M/M_{\odot}$ ,  $T_{\text{eff}}$ , and  $\log L/L_{\odot}$ , it is possible to identify the stars for which a problem with the stellar parameters is likely to be present, but this is not the case for any of our targets. The stars, falling above the equality line are:  $\gamma$  Ari, HD 43819, HD 47152, HD 116114, HD 130559, and HD 146001. For those stars the calculated  $\log g$  values are  $\leq 4.0$ , as expected for main sequence mCP stars, and therefore, we cannot exclude that their real rotational period is larger than that listed in Table 3. However, at least three objects ( $\gamma$  Ari, HD 47152, and HD 130559) were found to be part of close visual binaries (Horch et al. 2004; Mason et al. 2007). Hence, the brightness of the companion is included in the calculated luminosity, resulting into larger radii and thus smaller equatorial velocities. Since the brightness differences are not known, we are not able to apply the appropriate corrections.

## 5 CONCLUSION

We have analysed the light curves of 1028 chemically peculiar stars obtained with the *STEREO* spacecraft. In this work we presented the analysis and the results obtained for 337 magnetic chemically peculiar stars. The characteristics of the *STEREO* data allow the detection and study of photometric variations with periods between several hours and a few days and are therefore perfectly suitable to study rotational periods of mCP stars.

Using a matched filter algorithm we produced the light curve, phase-folded on the best fitting period, for each star and extracted from the whole sample the objects which appeared clearly constant, or too badly affected by systematic effects to allow any reliable analysis. Those stars are listed in Table 1.

For the remaining stars we performed a detailed analysis based on two different period finding algorithms and listed the objects we classified as constant in Table 2 and variable in Table 3. We detected relevant photometric variability and measured its period for 82 mCP stars. For 48 of them this work presents the first measurement of their rotation period, while for the remaining 34 our results are in agreement with previous estimations. It is important to notice that the stars we classified as constant, and therefore listed in

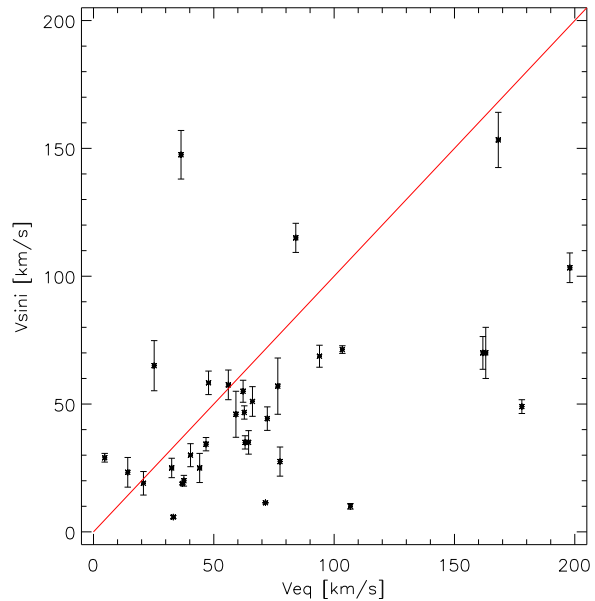


**Figure 10.** Comparison between the observed  $v \sin i$  and the computed  $V_{\text{eq}}$  for the stars listed in Table 3. The adopted  $v \sin i$  uncertainty is also listed in Table 3. The continuous line is the one-to-one relationship.

Table 1 and 2, might be intrinsically variable if their period is, for example, longer than 10 days or their light curve is affected by substantial blending or systematic effects. It is anyway likely that most of these stars are not chemically peculiar stars.

This work presents all the basic information necessary to plan detailed spectroscopic and/or spectropolarimetric observations for 82 mCP stars, e.g. to perform Doppler imaging. About half of them are only suspected mCP stars, for which no measurements of the magnetic field have been performed. These stars represent a good starting point for further spectropolarimetric observations to improve our statistics and knowledge of the complex phenomenon of magnetism in stars of the upper main sequence.

## ACKNOWLEDGMENTS

The Heliospheric Imager (HI) instrument was developed by a collaboration that included the Rutherford Appleton Laboratory and the University of Birmingham, both in the United Kingdom, and the Centre Spatial de Liège (CSL), Belgium, and the US Naval Research Laboratory (NRL), Washington DC, USA. The *STEREO*/SECCHI project is an international consortium of the Naval Research Laboratory (USA), Lockheed Martin Solar and Astrophysics Lab (USA), NASA Goddard Space Flight Center (USA), Rutherford Appleton Laboratory (UK), University of Birmingham (UK), Max-Planck-Institut für Sonnensystemforschung (Germany), Centre Spatial de Liège (Belgium), Institut d’Optique Théorique et Appliquée (France) and Institut d’Astrophysique Spatiale (France). This research has made use of the SIMBAD database, operated at CDS, Strasbourg, France. This research has made use of version 2.31 PERANSO light curve and period analysis software, maintained at CBA, Belgium Observatory <http://www.cbabelgium.com>. Astronomy research at the Open

University is supported by an STFC rolling grant (L.F.). KTW acknowledges support from a STFC studentship.

## REFERENCES

- Adelman, S. J. 2008, *PASP*, 120, 595
- Arenou, F., Grenon, M. & Gomez, A. 1992, *A&A*, 258, 104
- Babel, J. 1992, *A&A*, 258, 449
- Bagnulo, S., Landstreet, J. D., Mason, E., Andretta, V., Silaj, J. & Wade, G. A. 2006, *A&A*, 450, 777
- Bewsher, D., Brown, D. S., Eyles, C. J., Kellett, B. J., White, G. J. & Swinyard, B. 2010, *Solar Physics*, 264, 433
- Borra, E. F., Landstreet, J. D. & Thompson, I. 1983, *ApJS*, 53, 151
- Brown, D. S., Bewsher, D. & Eyles, C. J. 2009, *Solar Physics*, 254, 185
- Bychkov, V. D., Bychkova, L. V. & Madej, J. 2009, *MNRAS*, 394, 1338
- Bychkov, V. D., Bychkova, L. V. & Madej, J. 2005, *A&A*, 430, 1143
- Catalano, F. A. & Renson, P. 1998, *A&AS*, 127, 421
- Cutri, R. M., Skrutskie, M. F., van Dyk, S., et al., 2003, *2MASS All Sky Catalog of point sources. The IRSA 2MASS All-Sky Point Source Catalog*, NASA/IPAC Infrared Science Archive.
- Eyles, C. J., Harrison, R. A., Davis, C. J., et al. 2009, *Solar Physics*, 254, 387
- Glebocki, R., & Gnacinski, P. 2005, *ESA, SP-560*, 571, Vsini values
- Gomez, A. E., Luri, X., Grenier, S., Figueras, F., North, P., Royer, F., Torra, J. & Mennessier, M. O. 1998, *A&A*, 336, 953
- Harmanec, P. & Božić, H. 2001, *A&A*, 369, 1140
- Horch, E. P., Meyer, R. D. & van Altena, W. F. 2004, *AJ*, 127, 1727
- Kaiser, M. L., Kucera, T. A., Davila, J. M., St. Cyr, O. C., Guhathakurta, M. & Christian, E. 2008, *Space Science Reviews*, 136, 5
- Kharadze, E. K. & Chargeishvili, K. B. 1990, *AJ*, 379, 395
- Kharchenko, N. V. 2001, *Kinematika i Fizika Nebesnykh Tel*, 17, 409
- Kochukhov, O. & Bagnulo, S. 2006, *A&A*, 450, 775
- Koen, C. & Eyer, L. 2002, *MNRAS*, 331, 45
- Kraus, A. L., Craine, E. R., Giampapa, M. S., Scharlach, W. W. G. & Tucker, R. A. 2007, *AJ*, 134, 1488
- Kudryavtsev, D. O., Romanyuk, I. I., Elkin, V. G. & Paunzen, E. 2006, *MNRAS*, 372, 1804
- Kurtz, D. W. 1982, *MNRAS*, 200, 807
- Kurtz, D. W. 1989, *MNRAS*, 238, 1077
- Landstreet, J. D., Bagnulo, S., Andretta, V., Fossati, L., Mason, E., Silaj, J. & Wade, G. A. 2007, *A&A*, 470, 685
- Mason, B. D., Hartkopf, W. I., Wycoff, G. L. & Wieder, G. 2007, *AJ*, 134, 1671
- Mermilliod, J.-C., Mermilliod, M. & Hauck, B. 1997, *A&AS*, 124, 349
- Mikulášek, Z. 2007, *Astronomical and Astrophysical Transactions*, 26, 63
- Netopil, M., Paunzen, E., Maitzen, H. M., North, P. & Hubrig, S. 2008, *A&A*, 491, 545
- North, P. 1998, *A&A*, 334, 181
- Paunzen, E., Netopil, M., Pintado, O. I., Rode-Paunzen, M. 2011, *AN*, 332, 77
- Pourbaix, D., Tokovinin, A. A., Batten, A. H., et al. 2004, *A&A*, 424, 727
- Preston, G. W. 1974, *ARA&A*, 12, 257
- Renson, P. & Catalano, F. A. 2001, *A&A*, 378, 113
- Renson, P. & Manfroid, J. 2009, *A&A*, 498, 961
- Robitaille, T. P., Whitney, B. A., Indebetouw, R. & Wood, K. 2007, *ApJS*, 169, 328
- Romanyuk, I. I. & Kudryavtsev, D. O. 2008, *Astrophysical Bulletin*, 63, 139
- Samus, N.N., Durlevich, O.V., Kazarovets, E. V., Kireeva, N.N., Pastukhova, E.N., Zharova A.V., et al. *General Catalog of Variable Stars (GCVS database, Version 2011Jan)*
- Scargle, J. D. 1982, *ApJ*, 263, 835
- Schaerer, D., Charbonnel, C., Meynet, G., Maeder, A. & Schaller, G. 1993, *A&AS*, 102, 339
- Schlegel, D. J., Finkbeiner, D. P. & Davis, M. 1998, *ApJ*, 500, 525
- Shulyak, D., Tsymbal, V., Ryabchikova, T., Stütz Ch., & Weiss, W. W. 2004, *A&A*, 428, 993
- Skiff, B. A. 2010, *Catalogue of Stellar Spectral Classifications, VizieR On-line Data Catalog: B/mk*
- Stellingwerf, R. F. 1978, *ApJ*, 224, 953
- van Leeuwen, F. 2007, *A&A*, 474, 653
- Watson, C. L. 2006, *Society for Astronomical Sciences Annual Symposium*, 25, 47
- Wraight, K. T., White, G. J., Bewsher, D. & Norton, A. J. 2011, *MNRAS*, in press (arXiv: 1103.0911)

# A STEREO photometric study of chemically peculiar stars 11

Table 1: Basic properties of the CP2 and CP4 stars identified as constant or for which the quality of the data prevented the detection of any variability.

Name	# R09	RA deg.	DEC deg.	V mag	Spectral Type	CP class	$v \sin i$ km s <sup>-1</sup>
HD 965	160	3.51693	-0.03337	8.57	A8,Sr,Eu,Cr	CP2	90.0(13.5/1)
BD+09 124	1640	16.30230	10.27470	10.54	A0,NA	CP2	
HD 6590	1680	16.71320	15.74080	10.15	A3,NA	CP2?	
HD 17471	4380	42.19130	25.18810	5.89	A0,Si	CP2	46.3(1.2/3)
HD 20150	5000	48.72540	21.04440	4.88	A1,NA	CP2?	125.0(5.7/2)
HD 26571	6780	63.21350	22.41350	6.15	B8,Si	CP2	20.0(3.0/1)
HD 281886	6900	64.40670	31.43480	8.90	F0,Sr	CP2?	
HD 27295	7000	64.85870	21.14230	5.49	B9,Mn	CP2	9.2(0.5/6)
HD 284639	7770	71.49670	23.91680	9.63	A0,Si,Cr	CP2	
HD 32992	8440	76.93260	14.35960	8.19	A1,NA	CP2?	
AAO+32 27	8844	80.13170	32.60390	10.79	B9,Si	CP2?	
HD 242720	8858	80.22580	30.09630	10.60	B9,Si,Sr	CP2?	
HD 242705	8865	80.27430	32.43030	11.40	B9,Si	CP2?	
HD 243010	8951	80.70000	23.72580	10.80	A3,NA	CP2?	
HD 243202	8983	81.12300	32.81910	10.90	B5,NA	CP4	
HD 243308	9006	81.24240	30.07960	10.80	B9,Si	CP2?	
AAO+26 15	9028	81.29800	26.46530	10.90	B9,Si	CP2?	
BD+32 976	9024	81.32100	32.67810	10.27	A2,Sr	CP2?	
HD 243321	9026	81.32430	32.61640	9.64	A0,Si	CP2?	
HD 243395	9047	81.34460	29.36330	9.86	A0,Si,Sr	CP2?	
HD 243356	9034	81.36610	32.66690	11.60	A0,Si	CP2?	
HD 243408	9052	81.42580	32.30090	10.10	B9,Si	CP2?	
HD 35436	9059	81.53600	32.80490	9.57	A1,Si,Sr	CP2?	
HD 243492	9082	81.56870	33.26230	10.60	A0,Si,Sr	CP2?	
AAO+31 68	9155	81.73960	31.06840	11.54	B9,Sr	CP2?	
HD 35693	9220	81.80790	15.25760	6.18	A2,Cr	CP2?	77.5(8.0/2)
HD 243791	9215	81.95790	29.80130	11.40	A0,Sr	CP2?	
HD 243970	9246	82.28910	32.55970	10.07	B9,Si,Sr	CP2?	
HD 244099	9266	82.44620	31.63800	11.00	B9,Sr	CP2?	
AAO+31 112	9337	82.71830	31.26950	11.95	B8,Si	CP2?	
HD 244248	9336	82.72660	32.76810	11.40	A5,Si,Sr	CP2?	
AAO+28 89	9355	82.84630	28.23690	11.71	B9,Si,Sr	CP2?	
HD 244352	9351	82.85880	30.69890	10.70	B9,Si	CP2?	
HD 244876	9553	83.62420	29.26920	10.23	A0,Si,Sr	CP2?	
AAO+27 87	9572	83.65970	27.23250	10.70	B9,Si,Sr	CP2?	
HD 244933	9576	83.73770	32.56150	11.50	A1,Si	CP2?	
HD 244955	9613	83.76450	30.18470	12.10	A,Sr	CP2?	
HD 245112	9656	83.87710	23.28400	10.90	A0,Si,Cr	CP2?	
HD 245155	9662	83.92830	25.27480	9.86	B9,Si,Sr	CP2?	
HD 245153	9664	83.96980	28.16360	10.33	A0,Si,Sr	CP2?	
HD 245191	9698	84.07970	30.27230	11.20	A0,Si	CP2?	
HD 245222	9748	84.09270	27.90150	10.80	A5,Cr,Si	CP2?	
HD 245320	9837	84.21000	28.19000	10.56	B9,Si,Cr,Sr	CP2?	
HD 245353	9858	84.26490	27.62960	10.22	A1,Si,Sr	CP2?	
HD 245416	9876	84.38420	31.77830	9.43	A2,Cr,Si	CP2?	
HD 245725	10002	84.77580	32.63670	11.00	A0,Si	CP2?	
HD 245726	10008	84.78270	32.22540	10.80	A1,Si,Sr	CP2?	
HD 245786	10012	84.80020	29.05760	11.20	A,Si	CP2?	
HD 245990	10072	84.99170	26.37620	10.70	A1,Si	CP2?	
AAO+32 281	10047	85.00080	32.90320	11.22	B9,Si,Sr	CP2?	
HD 246148	10121	85.18930	23.52640	10.60	B9,Si	CP2?	
AAO+33 312	10107	85.25890	33.39200	11.30	B9,Si	CP2?	
HD 246276	10157	85.37980	25.99710	10.80	B9,Si	CP2?	
HD 246587	10224	85.71060	24.24100	11.00	A2,Si,Cr,Sr	CP2?	
HD 246685	10231	85.86690	27.47300	11.70	A,Si,Sr	CP2?	
HD 246861	10243	86.13330	28.53510	9.94	B9,Si	CP2?	
HD 246993	10258	86.21710	25.29510	10.80	B9,Si	CP2?	
HD 246970	10254	86.21970	28.56570	10.60	B9,Sr	CP2?	
AAO+30 227	10314	86.54500	30.92590	12.11	B9,Si,Sr	CP2?	
AAO+27 175	10323	86.62690	27.58840	11.63	B8,Si	CP2?	
AAO+29 209	10329	86.71300	29.56960	10.77	B8,Si,Cr	CP2?	
HD 247437	10332	86.79040	31.90220	10.04	B9,Si,Sr	CP2?	
HD 247591	10368	86.98250	29.49110	10.30	A1,Si,Cr,Sr	CP2?	
HD 247629	10379	87.09280	33.44420	10.80	A0,Sr	CP2?	
AAO+33 402	10381	87.09350	33.22400	11.92	B9,Si,Sr	CP2?	
HD 247794	10412	87.29340	32.47900	10.70	A0,Sr	CP2?	
HD 247833	10422	87.35370	32.83290	10.80	B9,Sr	CP2?	
HD 274959	10433	87.41930	26.94220	10.30	B9,Sr	CP2?	
HD 247931	10427	87.46170	33.45890	10.30	B7,Si	CP2?	
HD 248131	10463	87.69020	31.94080	10.60	B9,Si,Sr	CP2?	
AAO+31 309	10498	87.89430	31.74490	11.30	A2,Si	CP2?	
AAO+32 406	10509	88.00800	32.20760	11.62	A0,Sr	CP2?	
HD 39200	10513	88.04520	29.91650	9.33	B9,Si	CP2?	
HD 248582	10551	88.14810	24.22680	9.75	A0,Si	CP2?	
HD 248619	10561	88.26190	28.55520	10.67	B9,Si,Sr	CP2?	
HD 248727	10588	88.44110	33.28710	10.20	A0,Mn,Si,Cr	CP2?	
HD 248891	10603	88.62590	31.16230	10.05	A0,Si	CP2?	
HD 248943	10607	88.63820	28.90100	10.60	A0,Si	CP2?	

Table 1: continued.

Name	# R09	RA deg.	DEC deg.	V mag	Spectral Type	CP class	$v \sin i$ km s <sup>-1</sup>
HD 249121	10632	88.86340	24.03890	11.17	A1,Sr	CP2?	
HD 249279	10639	89.08810	28.73570	9.86	A0,Si,Sr	CP2?	
HD 249401	10663	89.25850	29.54600	10.80	A2,Si	CP2?	
HD 249478	10668	89.35870	29.88800	10.44	A1,Si,Sr	CP2?	
HD 40038	10669	89.42110	28.29090	8.55	A0,Sr	CP2?	
HD 249664	10697	89.56630	29.14840	10.65	A1,Si,Sr	CP2?	
AAO+28 373	10718	89.62280	28.73300	11.42	B8,Si,Sr	CP2?	
HD 249931	10793	89.95430	30.94990	10.60	A0,Si,Sr	CP2?	
AAO+28 401	10813	90.10110	28.70450	11.98	A0,Si	CP2?	
HD 250115	10819	90.15560	30.08410	10.14	B8,Si	CP2?	
HD 40678	10876	90.37170	23.70390	7.35	A0,Si,Sr	CP2	
HD 250515	10915	90.61390	28.49550	10.21	A0,Si	CP2?	
HD 250662	10931	90.71950	25.67540	8.96	B9,Si,Sr	CP2?	
AAO+28 455	10957	90.90330	28.53770	12.04	B8,Si	CP2?	
AAO+27 400	10965	90.94320	27.71830	11.28	B9,Si,Sr	CP2?	
HD 250827	10970	91.02330	32.88760	9.37	A3,Sr	CP2?	
HD 250962	11003	91.13700	30.23840	9.42	B9,Si	CP2?	
BD+25 1117	11094	91.60310	25.83430	10.80	B8,Si	CP2?	
HD 252076	11157	92.09630	23.92020	10.02	B8,Si,Sr	CP2?	
HD 252286	11186	92.28060	24.98930	10.20	A0,Sr	CP2?	
AAO+28 567	11196	92.45440	28.82590	11.72	B9,Sr	CP2?	
HD 252398	11194	92.50550	32.88770	9.67	B9,Cr,Si	CP2?	
HD 42477	11310	92.86630	13.63860	6.04	A1,Si	CP2	220.0(33.0/1)
HD 42509	11320	93.00560	19.79050	5.75	B9,Si	CP2?	92.5(9.0/2)
HD 259380	12410	98.49450	31.91610	10.62	A7,Sr	CP2?	
BD+21 1501	14670	106.32400	21.03770	10.30	NA,Si	CP2	
HD 68542	18990	123.47300	27.77860	7.77	F3-F7,Sr	CP2?	27.0(4.1/1)
HD 72943	20230	129.03200	15.31360	6.33	A5-F,NA	CP2?	63.7(1.4/4)
BD-02 3229	27140	162.39799	-3.38271	9.78	NA,Sr	CP2?	
HD 96097	27670	166.25400	7.33601	4.63	F3,Sr	CP2?	25.2(1.3/5)
HD 98664	28450	170.28400	6.02933	4.04	B9,Si	CP2?	60.6(0.4/5)
HD 104833	30360	181.07700	-9.35832	9.04	F0,Sr	CP2	40.4(1.7/1)
HD 109704	31810	189.19701	-5.83190	5.88	A2,NA	CP2	140.0(8.0/1)
HD 111702	32410	192.83299	-11.84510	8.81	F0,Sr	CP2	54.9(6.0/1)
HD 123255	35336	211.67799	-9.31351	5.46	F1,Cr	CP2?	154.7(9.4/5)
HD 134214	38100	227.25999	-13.99960	7.48	F2,Sr,Eu,Cr	CP2	
HD 142250	40360	238.62500	-27.33860	6.10	B6,He-weak	CP4	34.0(1.3/3)
HD 142502	40430	238.85800	-15.04090	9.50	A5,Sr,Eu	CP2	
HD 144941	41070	242.35201	-27.22730	10.02	B8,He	CP4?	
HD 146607	41420	244.56700	-30.95540	10.18	A0,Si	CP2	
HD 148117	41860	246.75800	-26.74220	10.70	A7,Si,Eu,Cr	CP2	
HD 149151	42180	248.54601	-31.28480	8.12	A0,Si	CP2	
HD 150347	42510	250.39799	-28.58640	8.97	B9,Si	CP2	
HD 151560	42870	252.31400	-28.71010	9.73	A3,Sr	CP2	
HD 192723	53790	304.34100	-28.49830	10.41	A0,Si	CP2	
HD 196691	54900	309.79400	-6.15760	8.63	A0,Si	CP2?	
BD-12 5801	54930	310.07199	-12.23580	9.70	NA,Sr	CP2	
HD 198216	55190	312.24700	-5.74948	9.94	A0,NA	CP2?	
HD 202406	56400	318.97900	-9.39114	7.85	F2,Sr	CP2	
HD 207052	57620	326.63400	-11.36600	5.57	A1,NA	CP2	192.5(5.7/2)
HD 209051	58130	330.16699	-6.43251	8.76	A0,Si,Cr,Eu	CP2	
HD 215624	59570	341.67200	-13.55160	10.56	A2,Sr,Si	CP2?	
HD 216018	59680	342.35999	-11.34920	7.61	A7,Sr,Eu,Cr	CP2	
HD 219831	60350	349.75601	-9.05975	10.10	A2,Sr	CP2	
HD 222962	61143	356.34100	10.17980	6.55	A4,NA	CP2?	

Table 2: Basic properties of the CP2 and CP4 stars identified as constant or probably constant after the individualised analysis. The relevant references are given at the end of Table 3.

Name	# R09	RA deg.	DEC deg.	V mag	Spectral Type	CP class	Period days	$\sigma_{period}$ days	Analysis remarks	Literature period	$v \sin i$ km s <sup>-1</sup>
HD 224926	61680	0.45603	-3.02750	5.12	B8,He-weak,Mn	CP4	3.1604	0.0036	BW		67.5(6.4/2)
HD 1758	402	5.45132	0.91719	9.13	A2,Sr	CP2	1.4482	0.0016	W		
HD 10809	2680	26.47920	3.41756	6.82	A8,Sr,Cr,Eu	CP2			C	K07:2.693	
HD 22374	5660	54.24180	23.21110	6.73	A1,Cr,Sr,Si	CP2			B	C98:10.6	5.0(0.8/1)
HD 23387	5980	56.40740	24.33560	7.19	A0,Cr,Si	CP2			B		23.5(2.1/2)
HD 23850	6100	57.29060	24.05340	3.62	B8,He-weak	CP4	2.4624	0.0016	BW		182.5(18.0/2)
HD 23964	6140	57.49190	23.84870	6.74	B9,Si,Sr,Cr	CP2	1.5814	0.0008	BW		39.0(2.8/2)
HD 27778	7120	65.99070	24.30390	6.33	A1,Si	CP2			B		
GSC 02390-00208	8795	79.75760	30.10350	10.80	A2,Si,Sr	CP2?	1.8444	0.0019	W		
HD 242692	8847	80.22540	33.08600	9.65	B9,Si	CP2	0.6180	0.0001	BW		
HD 242800	8891	80.40920	32.75880	10.30	A0,Si	CP2?			B		
HD 243007	8954	80.78520	30.22440	10.20	A1,Si	CP2?			C		
GSC 02394-00537	8947	80.78660	32.52450	10.90	B9,Si	CP2?			C		
AAO+27 25	9058	81.40010	27.07680	11.61	A0,Si,Sr	CP2?	2.4922	0.0009	W		
HD 243378	9048	81.40560	33.26270	10.90	A0,Si,Sr	CP2?			C		
AAO+33 110	9051	81.42540	33.31920	11.33	B9,Si,Sr	CP2?			C		
HD 243494	9080	81.55130	32.03430	9.68	B9,Si	CP2			B		
GSC 02403-00597	9104	81.58790	31.21740	11.40	A0,Si,Cr,Sr	CP2?	2.7865	0.0029	BW		
AAO+30 76	9132	81.62010	30.36130	11.33	A0,Sr	CP2			B		
HD 243523	9106	81.62030	33.30000	11.10	A0,Si,Sr	CP2			B		
HD 243954	9240	82.21120	29.04410	9.97	A1,Si	CP2			C		
HD 244303	9345	82.80410	32.71930	11.40	A,Sr	CP2?			C		
AAO+32 173	9348	82.83030	32.61440	11.89	B9,Si	CP2?			C		
HD 244372	9354	82.88850	31.63940	10.60	A1,Sr	CP2?			C		
HD 244391	9357	82.92280	31.62360	10.40	B8,Si,Sr	CP2?			C		
HD 244531	9376	83.14980	33.24090	11.45	B9,Si	CP2?			C		
HD 244737	9485	83.48850	32.99670	11.00	A0,Si	CP2?			C		
BD+26 859	9626	83.78830	26.22660	10.70	B8,Si,Sr	CP2?			C		
BD+23 959	9792	84.09180	23.60270	10.25	A0,Si	CP2?			C		
AAO+28 129	9833	84.19650	28.18920	11.59	B9,Sr	CP2?			C		
HD 37098	9865	84.28690	26.92430	5.83	B9,Si	CP2			B		50.0(7.5/1)
HD 245423	9872	84.31840	27.26770	10.55	A3,Si	CP2?			C		
GSC 01873-00586	9953	84.53710	29.01000	9.86	B9,Si,Sr	CP2?			C		
HD 245839	10033	84.85310	28.65370	10.90	A1,Si	CP2?			C		
GSC 01873-00024	10108	85.19830	28.77060	11.00	B9,Si	CP2?			C		
HD 246380	10178	85.54000	29.25040	9.50	B8,Si,Sr	CP2?			C		
GSC 01870-00880	10233	85.88120	27.17130	10.70	A1,Si	CP2?			C		
HD 246820	10239	86.06830	27.95520	10.70	A0,Si,Sr	CP2?			C		
GSC 01870-01556	10302	86.39660	27.57710	10.50	A0,Sr	CP2?			B		
GSC 01870-01678	10308	86.45320	27.70060	11.10	A0,Sr	CP2?			B		
GSC 02405-00885	10317	86.60060	31.27390	10.70	A2,Si,Cr	CP2?			B		
AAO+24 194	10333	86.71400	24.51800	12.13	A2,Si,Sr	CP2?			B		
AAO+27 185	10365	86.93900	27.16750	11.95	B9,Sr	CP2?	1.5409	0.0006	BW		
HD 247664	10385	86.98800	23.83660	10.40	B9,Si,Sr	CP2?			B		
HD 247607	10372	87.00810	29.82130	10.60	B9,Sr	CP2?			C		
AAO+31 260	10373	87.03770	31.41910	11.16	B9,Si,Sr	CP2?			C		
HD 248072	10447	87.51170	23.67330	10.50	B9,Si,Cr	CP2?			C		
AAO+31 290	10449	87.62550	31.58220	11.60	B9,Sr	CP2?			B		
GSC 01875-00443	10572	88.31570	29.68850	11.00	B9,Si	CP2?			C		
HD 248815	10596	88.42090	23.45250	10.57	B9,Si	CP2?			B		
HD 248767	10591	88.42370	28.67700	10.13	A0,Si,Cr,Sr	CP2?			C		
HD 248769	10594	88.43610	27.41140	10.00	B8,Si,Sr	CP2?			B		
AAO+28 312	10595	88.46310	28.37830	10.93	B9,Si,Sr	CP2?			B		
HD 248944	10609	88.66830	28.07180	10.20	A1,Si,Sr	CP2?			B		
AAO+27 276	10633	88.90310	27.31990	10.94	B8,Si	CP2?			C		
HD 39865	10643	89.12840	29.75200	8.61	B8,Si	CP2?	0.9186	0.0002	BW		
AAO+30 338	10661	89.24500	30.90880	11.77	B8,Si,Sr	CP2?	3.4992	0.0027	BW		
GSC 02406-01432	10662	89.26840	31.21150	10.90	A0,Si	CP2?			B		
AAO+28 354	10664	89.28640	28.10530	9.56	B9,Sr	CP2?			B		
GSC 01867-02081	10729	89.69550	25.93460	11.50	B9,Si,Sr	CP2?			C		
HD 250027	10805	90.04370	28.57790	10.17	A1,Si,Sr	CP2?			C	S+W:19.7803	
HD 250149	10825	90.20590	30.75830	10.50	B9,Si,Sr	CP2?			C		
HD 41055	10973	91.00220	28.64630	8.80	B9,Si	CP2?			C		
GSC 01868-00948	11023	91.21190	25.82570	11.50	B9,Si,Sr	CP2?			C		
HD 41282	11031	91.28880	24.34480	8.65	B9,Si	CP2?			B		
HD 251408	11084	91.53450	27.81520	10.70	A1,Si,Cr,Sr	CP2?			B		
HD 41418	11087	91.56510	27.93470	8.64	A0,Si	CP2?			B		
HD 251621	11105	91.66430	24.28540	9.97	A0,Sr	CP2?			B		
GSC 01872-02444	11101	91.67110	27.75790	10.50	A0,Si,Sr	CP2?			B		
HD 251582	11104	91.68080	26.17420	10.38	A3,NA	CP2?			B		
HD 251784	11113	91.86190	26.02850	10.13	A2,NA	CP2?			C		
HD 251947	11131	91.94900	23.19990	10.95	A2,NA	CP2?			B		
HD 251879	11122	91.95200	26.32510	10.80	B9,Sr	CP2?			B		
AAO+27 454	11136	92.03300	27.55900	11.67	A0,Si,Sr	CP2?			B		
HD 252106	11162	92.09440	23.62650	10.66	A0,Si	CP2?			B		
GSC 00742-02169	11180	92.10050	13.94660	10.80	A0,Si	CP2	1.4828	0.0004	BW	C01:1.563	
HD 252104	11168	92.12350	25.09050	10.50	B9,Si,Sr	CP2?			B		
AAO+27 460	11166	92.15390	27.62310	11.17	A0,Si	CP2?			C		

Table 2: continued.

Name	# R09	RA deg.	DEC deg.	V mag	Spectral Type	CP class	Period days	$\sigma_{period}$ days	Analysis remarks	Literature period	$v \sin i$ km s <sup>-1</sup>
HD 41869	11177	92.16520	25.65730	9.04	B9,Si	CP2			B		
HD 252459	11230	92.44260	24.22580	10.50	A,Si	CP2?			B		
AAO+24463	11271	92.55130	24.14160	11.41	B9,Si	CP2?			C		
AAO+24467	11272	92.55850	24.41250	10.55	B9,Si	CP2?			B		
BD+23 1328	11810	95.74010	23.27380	10.30	A2,Sr	CP2			C		
HD 44903	11880	96.33670	23.05680	8.39	A5,Sr,Eu	CP2			B		
HD 47103	12630	99.43360	19.94860	9.15	A,Sr,Eu	CP2			C		
HD 263361	13070	101.49600	19.16200	9.27	B9,Si	CP2			B		
HD 48953	13123	101.70600	16.77250	6.81	F,Sr,Eu	CP2	2.8939	0.0024	BSW		
HD 50403	13790	103.51500	22.26250	9.23	A2,Sr,Eu	CP2			C		
BD+23 1580	14530	105.97100	23.07520	9.83	A2,Cr,Eu	CP2?	2.4674	0.0019	BW		
GSC 01909-01687	15650	110.32900	22.57300	10.50	NA,Sr	CP2			B		
HD 62510	17130	116.28900	20.31600	6.54	A0,Si	CP2?			B		100.0(9.5/2)
HD 72359	20027	128.16600	10.06600	6.48	A1,Sr	CP2?			CS		19.0(4.0/4)
GSC 01398-00532	20050	128.33501	20.40690	11.40	NA,He	CP4?	3.9607	0.0053	BW		
HD 94603	27300	163.82100	-1.42467	9.35	A0,Sr,Eu,Cr	CP2			C		
HD 96003	27650	166.13901	12.66700	6.87	A3,Sr,Cr	CP2			B		
HD 109860	31890	189.51801	3.28245	6.33	A1,Si	CP2?			CS		62.1(2.0/5)
HD 112118	32560	193.56799	-10.66760	10.23	A0,Cr,Eu	CP2?			B		
HD 118054	34040	203.66901	-13.21430	5.92	A1,Sr,Eu,Cr	CP2?	1.7912	0.0010	BW		54.0(5.7/2)
HD 125248	35760	214.65900	-18.71600	5.85	A1,Eu,Cr	CP2	9.3105	0.0130	SW	C01:9.295	12.5(5.7/2)
HD 126365	36018	216.34900	-14.08500	8.47	F0,Sr,Cr	CP2			C		
HD 138426	39420	233.14200	-19.40270	8.57	B9,Sr,Cr	CP2	1.6571	0.0008	SW		
HD 138633	39460	233.39200	-11.06520	8.63	F0,Sr,Eu,Cr	CP2			C		
HD 139160	39630	234.36900	-26.27990	6.19	B7,He-weak	CP4?	6.2609	0.0218	BW		50.0(1.3/5)
HD 143517	40675	240.39400	-21.72100	9.57	A3,Sr	CP2			B		
HD 144748	41020	242.08701	-25.12720	8.60	F0,Sr,Eu,Cr	CP2	3.9815	0.0062	BW		
HD 146254	41360	243.96500	-14.84910	6.09	A0,Si	CP2?			C		137.5(14.3/2)
HD 146998	41520	245.04100	-25.85730	9.65	A6,Sr,Cr	CP2			C	C98:1.2	25.0(3.8/1)
HD 148321	41900	247.06300	-25.45400	6.97	A1-A8,Sr	CP2			C		55.0(8.3/1)
HD 148593	42010	247.41400	-14.58510	9.13	A2,Sr	CP2			B		
GSC 06807-00646	42000	247.53200	-28.56320	10.70	NA,Si	CP2			C		
HD 149228	42200	248.60100	-25.54970	10.06	B9,Si	CP2			C		
HD 150035	42440	249.88200	-27.28560	8.71	A3,Cr,Eu,Sr	CP2	2.3389	0.0013	W	C98:0.54	75.0(11.3/1)
HD 150715	42645	250.94800	-25.21780	10.13	A0,Sr,Cr,Eu	CP2			C		
HD 151941	42980	252.90500	-26.68970	9.91	A7,Sr,Eu,Cr	CP2	0.0659	0.0001	BW		
HD 191430	53330	302.56201	-13.01010	8.41	A7,Sr,Eu,Cr	CP2			B		
HD 191695	53430	303.01001	-21.30080	9.87	A3,Sr,Eu,Cr	CP2			B		
HD 196470	54770	309.54099	-17.50180	9.72	A2,Sr,Eu	CP2			B		
HD 206088	57390	325.02301	-16.66230	3.68	A7-F3,Sr	CP2			S		34.5(1.9/4)
HD 206103	57400	325.02499	-11.32830	9.47	A0,Si	CP2			C		
HD 207969	57820	328.34000	-14.18930	8.16	A7,Sr,Eu,Cr	CP2			CS		
HD 215766	59600	341.92801	-14.05640	5.68	B9,Si	CP2?	5.2310	0.0087	BSW		80.0(12.0/1)
HD 215913	59640	342.16501	-2.15105	9.71	A0,Sr,Eu,Cr	CP2	1.8396	0.0010	BSW		



Table 3. *Continued*

HD 141249	40104	237.16800	-18.41120	10.19	A3,Sr,Eu	CP2	1.2297	0.0004	54383.641	B									
HD 142096	40340	238.33400	-20.16700	5.03	B3,He-weak	CP4	3.3136	0.0032	54387.383	S		175.0(13.4/3)	16478(131/4)	2.62(0.14/Z)	4.65(0.27)	0(0)			
							0.5836	0.0001											
HD 142301	40380	238.66499	-25.24370	5.87	B8,He-weak,Si	CP2	1.4596	0.0004	54387.047	B*	C01:1.4595 / S+W:1.45937 / B:1.45955	B:2103	68.7(4.3/3)	15860(150/99)	2.62(0.13)	4.54(0.22)	0.16(0.22)		
HD 142884	40510	239.45300	-23.52730	6.78	B9,Si	CP2	0.8030	0.0002	54389.202	S*		B:285	155.0(18.4/2)	14223(270/4)	2.17(0.14/Z)	3.63(0.19)	0(0)		
HD 142990	40530	239.64500	-24.83150	5.43	B6,He-weak	CP4	0.9789	0.0003	54387.177	*	C01:0.979 / S:0.492 / B:0.9791	B:1304	153.3(10.8/3)	17700(1130/99)	2.97(0.10)	5.55(0.28)	0.30(0.27)		
HD 145102	41120	242.56599	-26.90910	6.59	B9,Si	CP2	1.4178	0.0006	54390.576	*		B:281	71.3(1.5/4)	10919(182/4)	2.03(0.15)	2.95(0.18)	0.63(0.21)		
HD 145501	41240	242.99400	-19.45020	6.26	B9,Si	CP2	0.5853	0.0001	54388.737	B		B:1242	60.0(9.0/1)	13715(156/2)		4.41(0.88)			
							0.7323	0.0001											
HD 145792	41280	243.43900	-24.42240	6.40	B6,He-weak	CP4?	1.6956	0.0005	54389.824	B*	W:0.8478	B:286	25.7(2.3/3)	14710(143/4)	2.33(0.15/Z)	3.90(0.23)	0(0)		
HD 146001	41310	243.72301	-25.47700	6.06	B8,He-weak	CP4?	3.9146	0.0041	54392.197	B*		B:647	147.5(9.5/2)	13790(300/99)	2.41(0.12)	3.84(0.21)	0.40(0.29)		
							0.5577	0.0001											
HD 147010	41530	245.02299	-20.05640	7.40	B9,Si,Cr,Sr	CP2	3.9209	0.0048	54394.083	B*	C01:3.9207 / B:3.920676	B:4032	26.5(2.7/2)	12752(219/4)	2.00(0.18/Z)	3.18(0.20)	0(0)		
HD 147105	41560	245.20500	-25.39430	8.82	A3,Sr,Cr,Eu	CP2	2.0025	0.0008	54392.388	B*	C98:1.9	B:456	50.0(7.5/1)	8200(269/3)		2.23(0.45)			
HD 147890	41720	246.41299	-29.40040	7.67	A0,Si,Sr	CP2	4.3359	0.0059	54395.777	*	C01:4.336	B:235	46.7(2.6/3)	11329(300/4)	2.63(0.38)	3.90(0.53)	0.97(0.13)		
HD 150714	42640	250.91499	-22.73650	7.59	A0,Si	CP2	1.6290	0.0008	54396.038	B*	C01:1.6288			10547(60/4)	1.71(0.19)	2.58(0.18)	0.30(0.31)		
HD 150716	42650	250.96400	-25.77780	9.70	A0,Si	CP2	1.9899	0.0013	54396.727	B*				11368(42/2)		3.33(0.64)			
HD 151346	42810	251.94400	-23.97430	7.91	B7,He-weak	CP4	2.1797	0.0017	54398.734			B:245	46.0(9.0/1)	14404(187/2)	2.40(0.21)	3.94(0.31)	0.19(0.29)		
HD 190576	52978	301.55801	-19.49040	7.64	B9,Si	CP2	0.5063	0.0001	54095.403	B				12352(-/1)		3.76(0.74)			
HD 191287	53290	302.42499	-18.34670	8.22	B9,Eu	CP2	1.6235	0.0007	54096.503	*	C01:1.6234			11445(-/1)	2.08(0.37)	3.08(0.45)	0.57(0.43)		
HD 199728	55630	314.90100	-19.03530	6.27	B9,Si	CP2	2.2411	0.0011	54112.643	*	C01:2.241 / S:2.25	R:400	57.5(5.8/2)	11935(114/3)	2.05(0.13)	3.11(0.16)	0.37(0.27)		
HD 207188	57640	326.90201	-17.29470	7.64	A0,Si	CP2	2.6733	0.0022	54124.810	*	S:2.67	K:1220	30.0(4.5/1)	12303(35/3)	1.78(0.22/Z)	2.91(0.20)	0(0)		
HD 210424	58510	332.65601	-11.56490	5.44	B6,Si	CP2	3.9613	0.0033	54128.906	B				20.0(2.1/2)	12662(257/3)	2.30(0.11)	3.53(0.16)	0.54(0.19)	
HD 211099	58630	333.72501	-6.73547	7.64	B9,Si	CP2	3.7887	0.0042	54132.431	*				12396(106/3)	2.37(0.39)	3.59(0.58)	0.67(0.42)		
HD 220825	60520	351.73300	1.25561	4.95	A1,Cr,Sr,Eu	CP2	1.4150	0.0005	54149.117	*	C01:1.41 / S:0.58525 / B:1.14077	B:269	35.0(4.6/3)	9200(80/99)	1.32(0.09)	2.09(0.09)	0.20(0.23)		
HD 224103	61430	358.78201	7.07097	6.22	A0,Si	CP2?	2.5341	0.0023	54503.094					10460(156/4)	1.72(0.11)	2.58(0.13)	0.36(0.28)		

B(period): Bychkov et al. (2005)

B(magnetic field): Bychkov et al. (2009)

C98: Catalano &amp; Renson (1998)

C01: Renson &amp; Catalano (2001)

K: Kudryavtsev et al. (2008)

KE: Koen &amp; Eyer (2002)

K07: Kraus et al. (2007)

R: Romanyuk &amp; Kudryavtsev (2008)

S: Samus et al. (2009)

W: Watson (2006)



This paper has been typeset from a  $\text{T}_{\text{E}}\text{X}/\text{L}_{\text{A}}\text{T}_{\text{E}}\text{X}$  file prepared by the author.

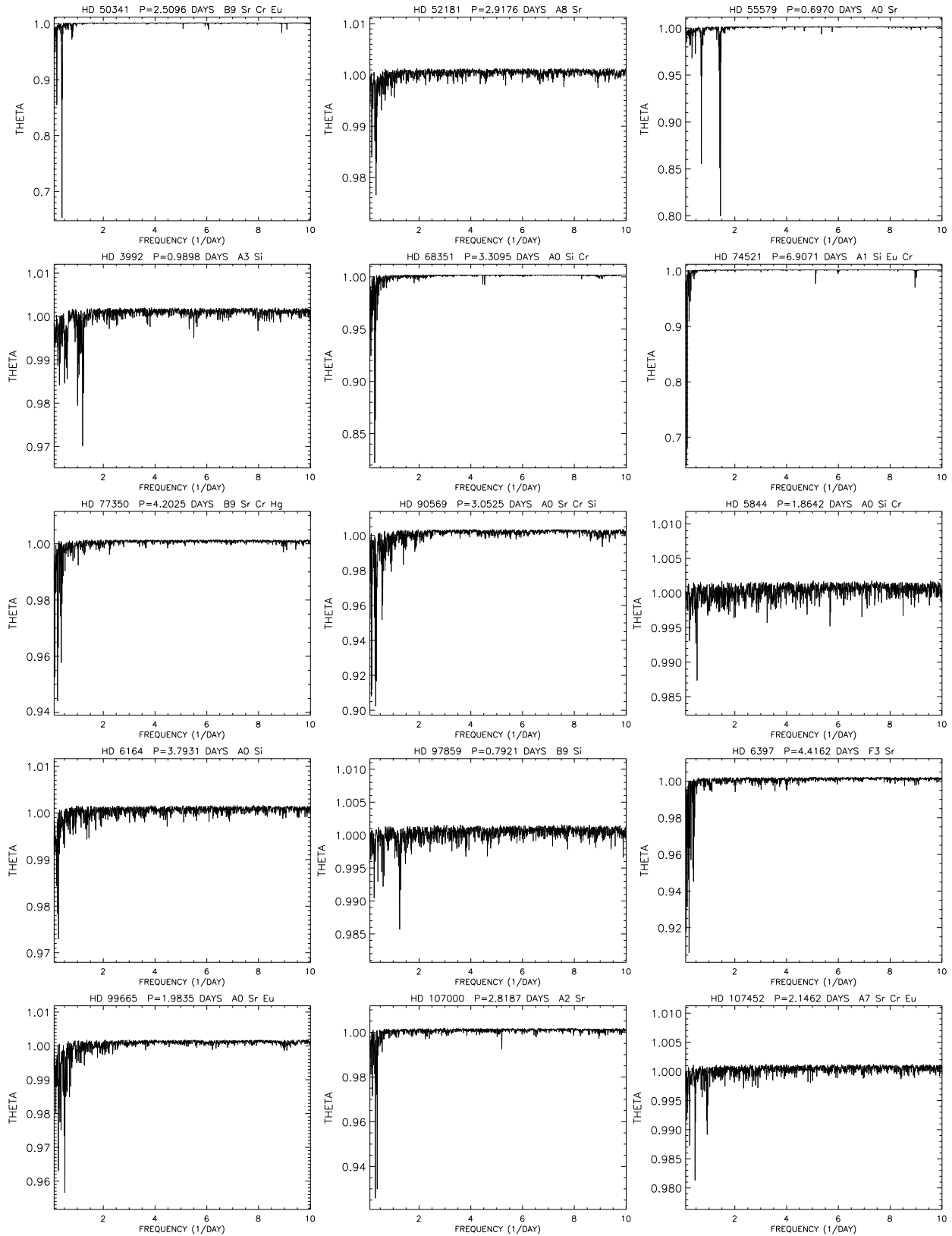
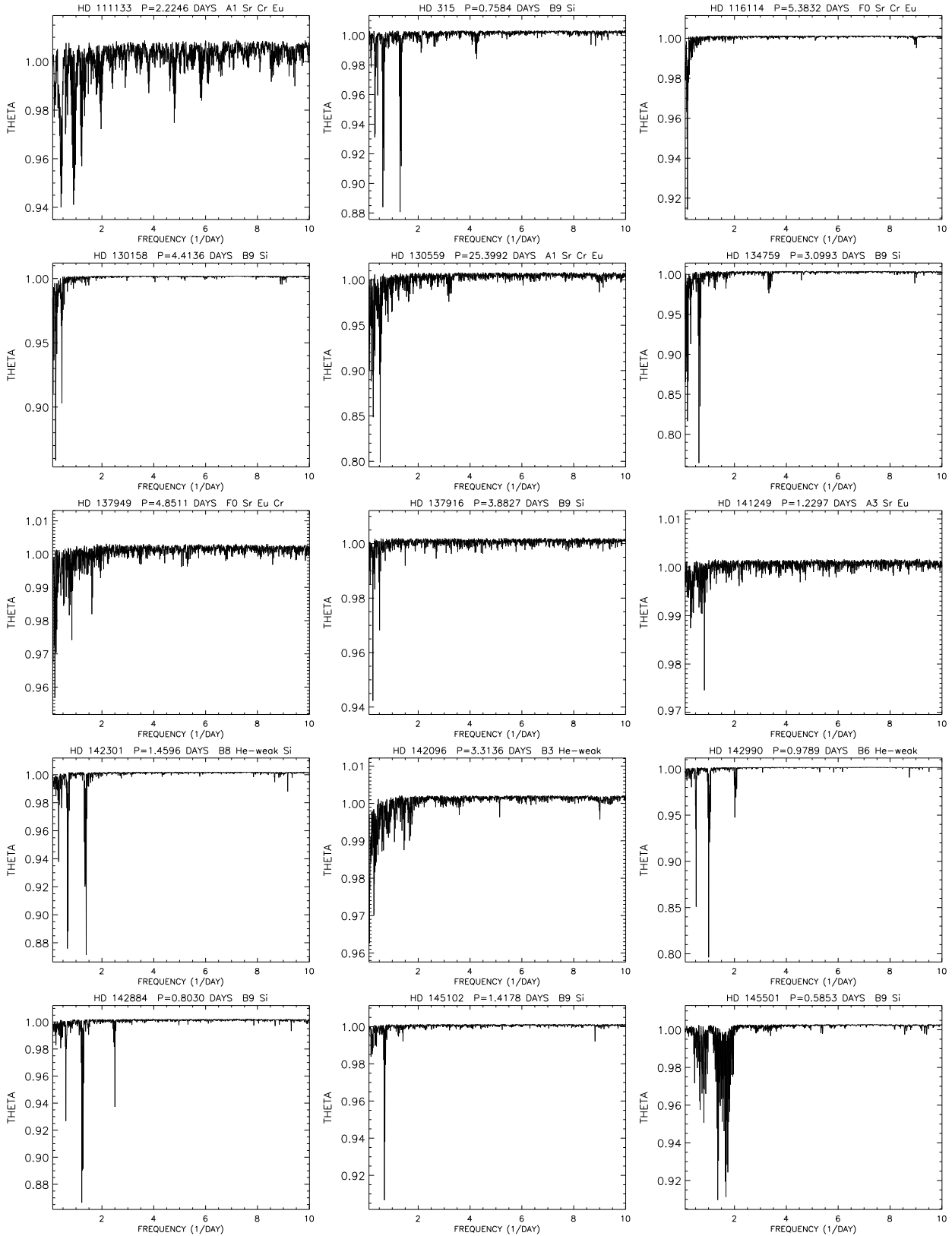
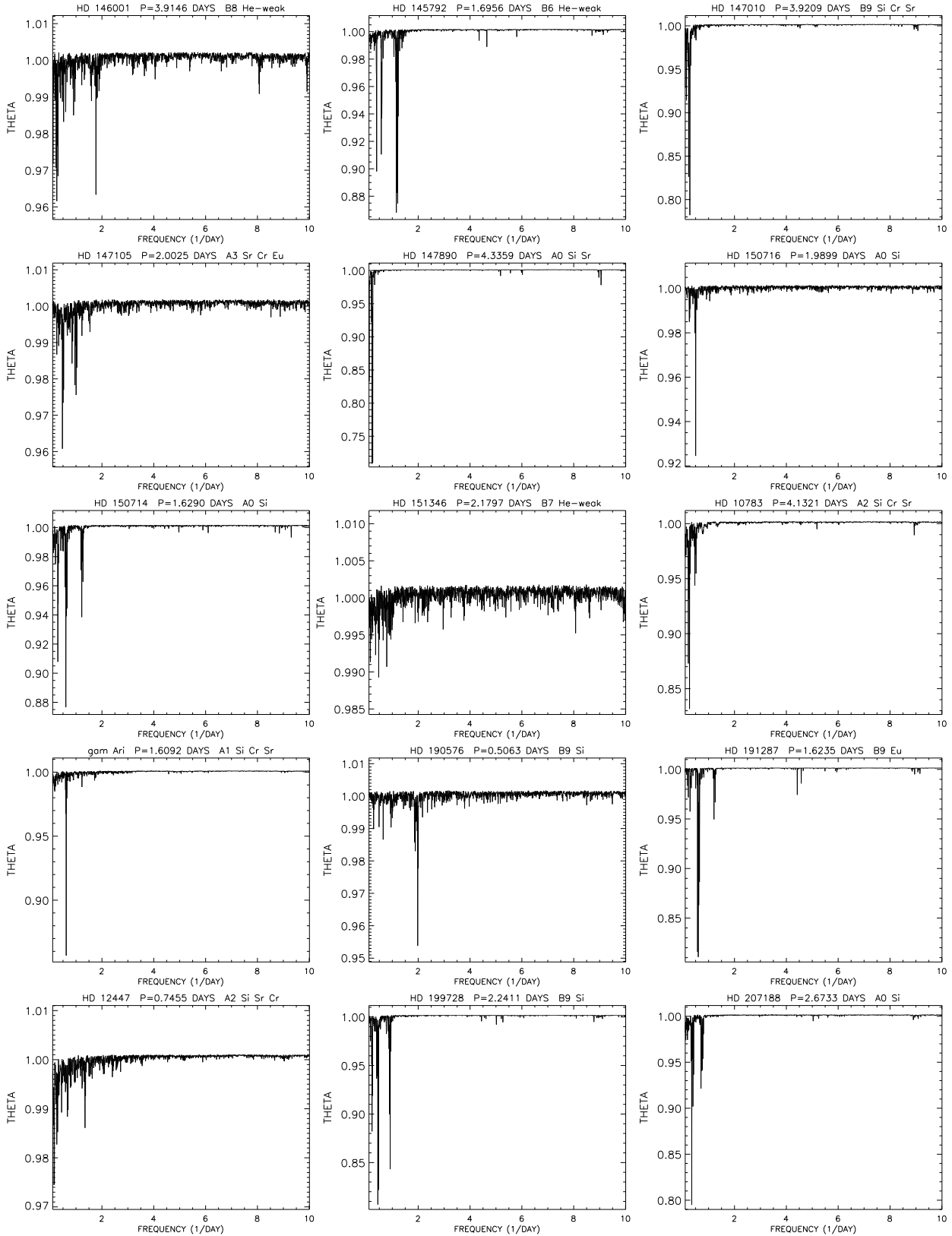
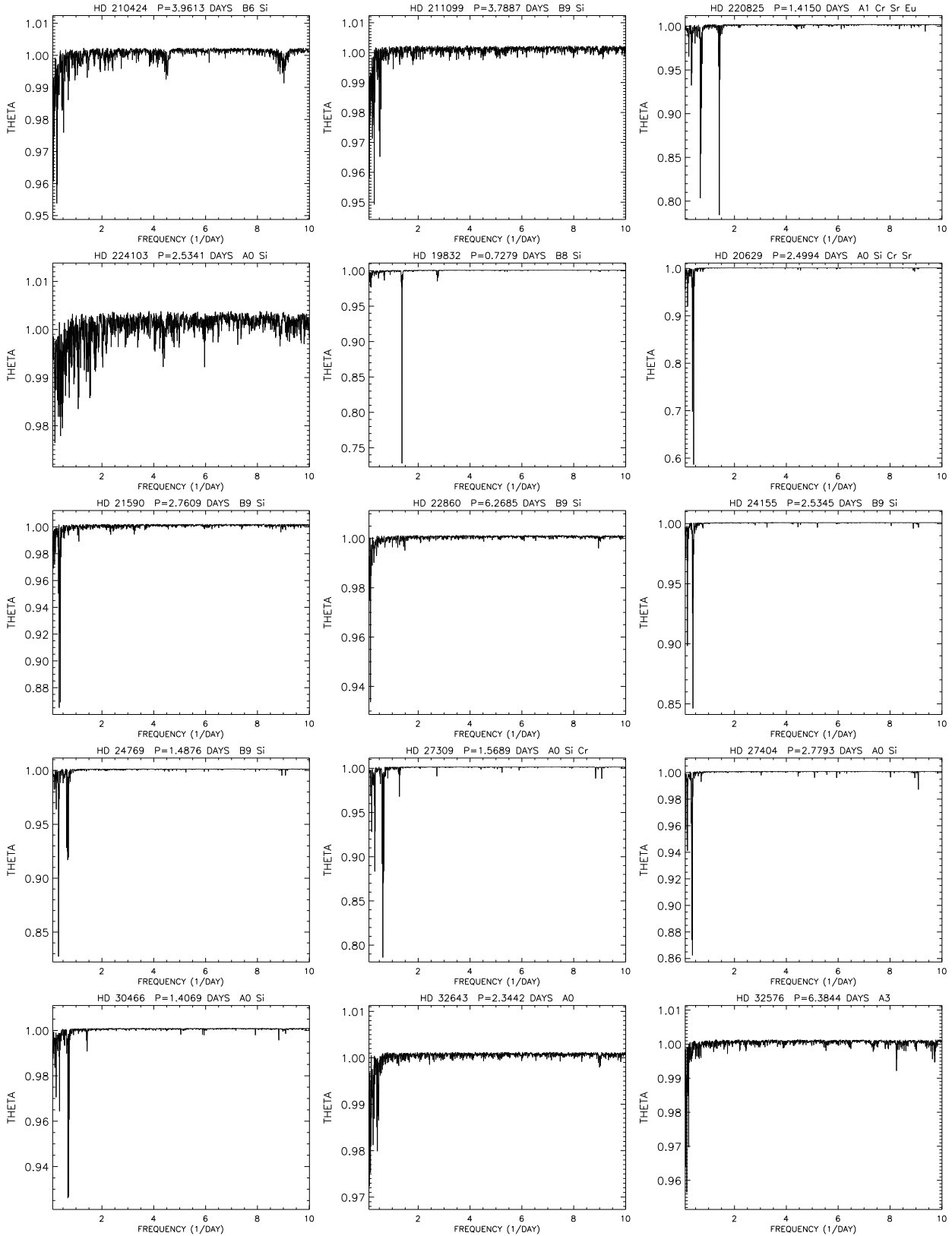
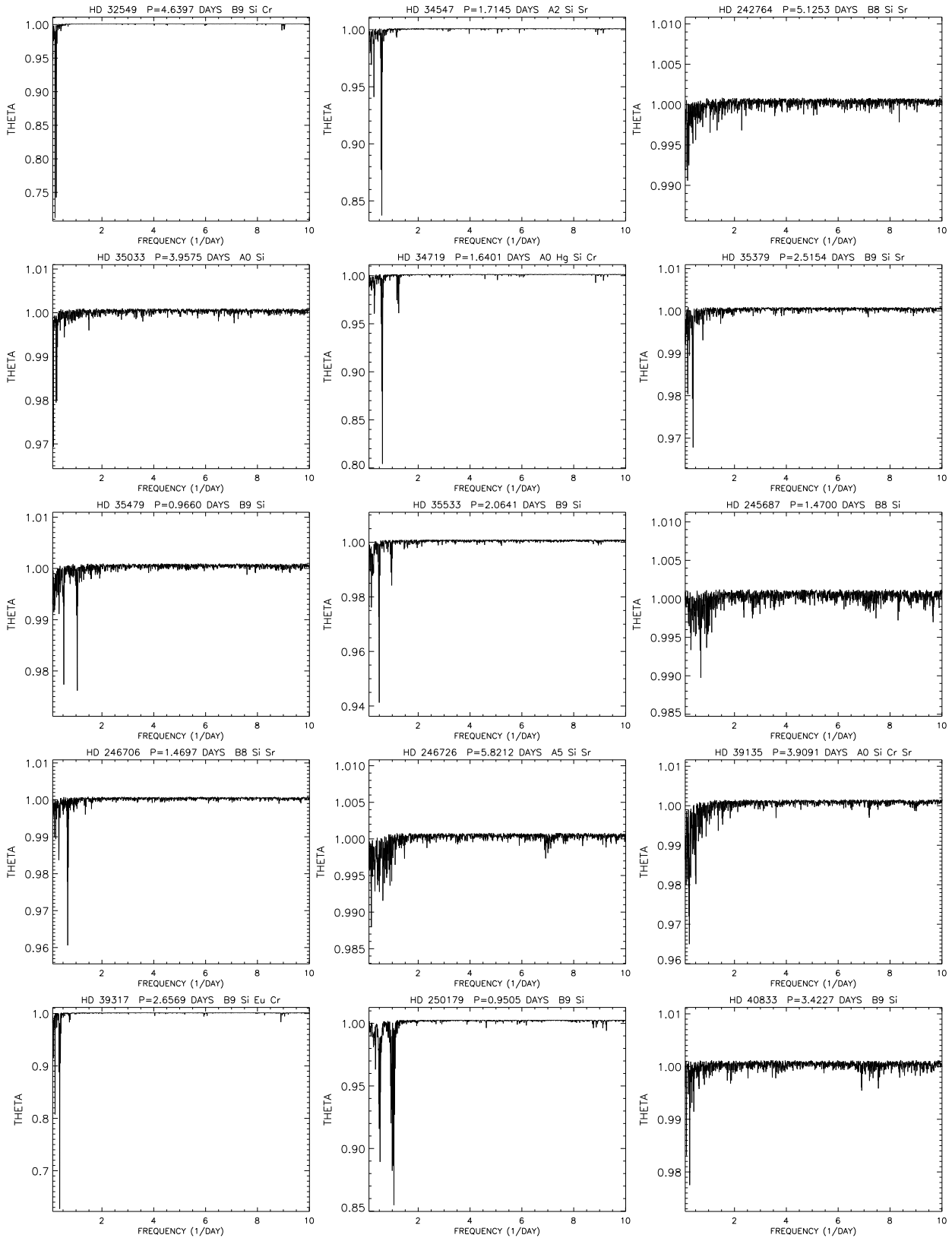


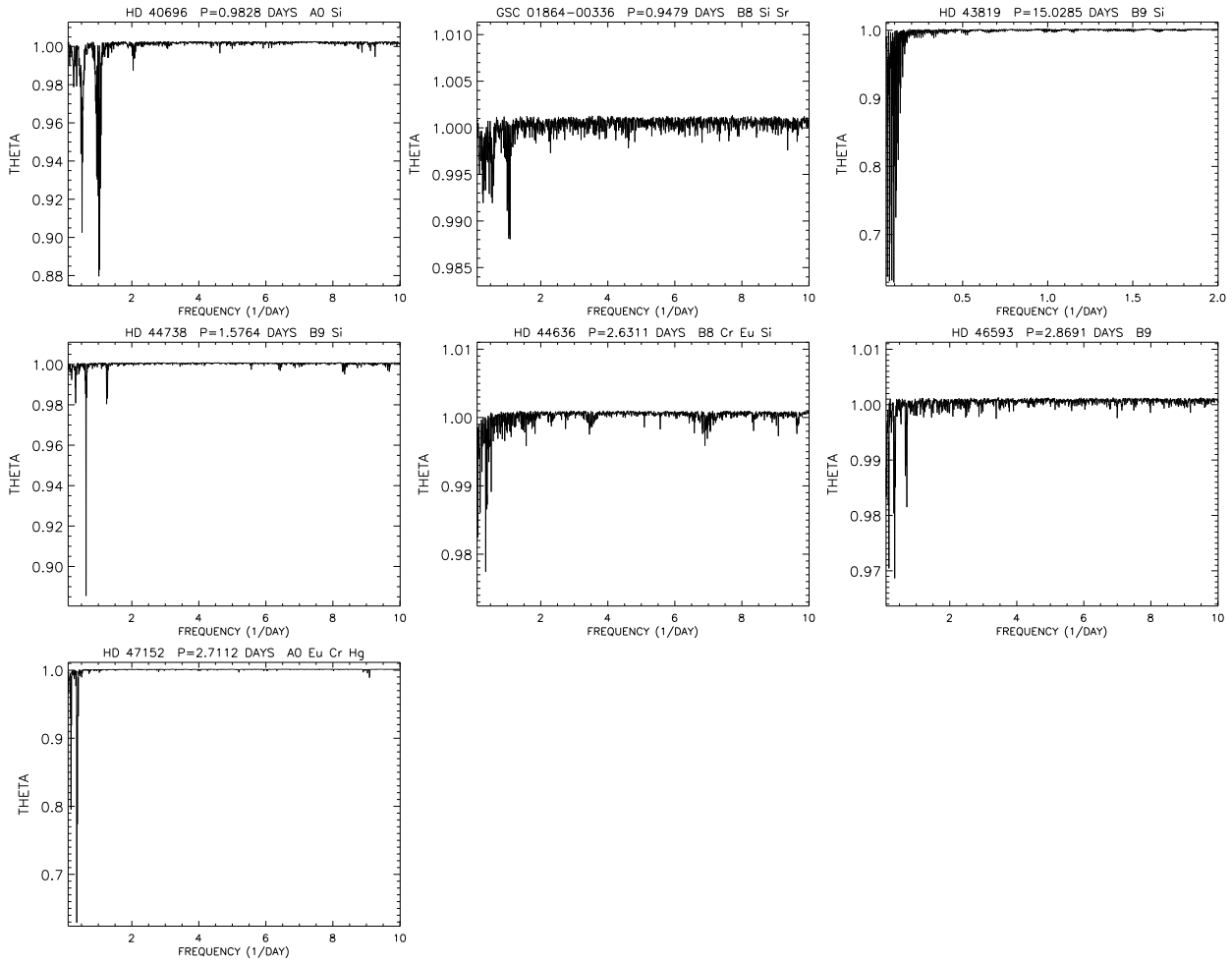
Figure 11. Periodograms obtained for the mCP stars, listed in Table 3.











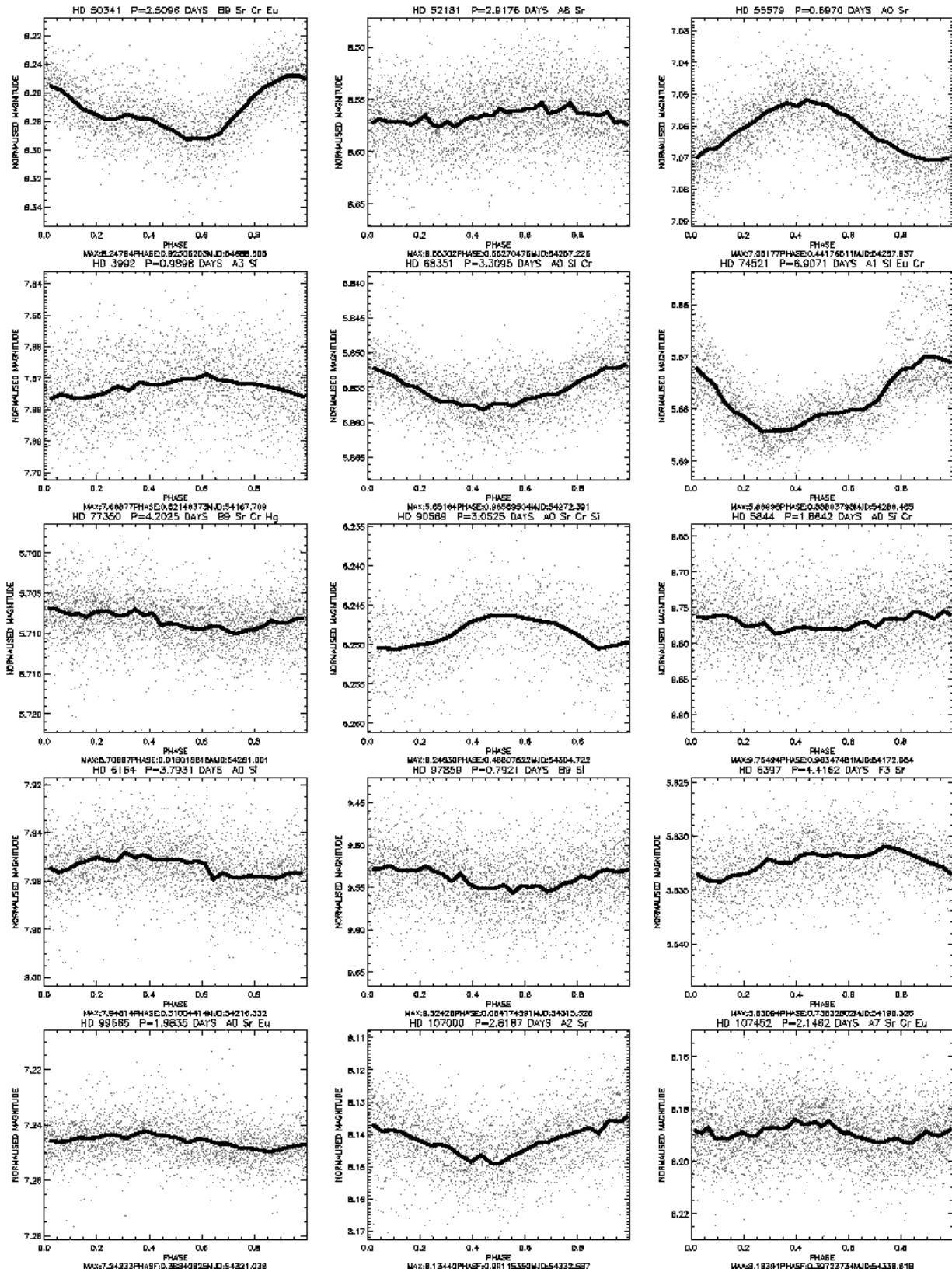


Figure 12. Light curves obtained for the mCP stars, listed in Table 3, phase-folded on the most significant period.



